A SUBSIDENCE, COMPACTION, PRESSURE, TEMPERATURE, AND MATURITY HISTORY OF THE HIBERNIA B-08 WELL, GRAND BANKS OF NEWFOUNDLAND

Kevin Joseph DesRoches

Submitted in Partial Fulfilment of the Requirements

for the Degree of Bachelor of Science, Honours

Dalhousie University, Halifax, Nova Scotia

April, 1992

Dalhousie University

Department of Earth Sciences
Halifax, Nova Scotia
Canada B3H 3J5
(902) 494-2358
FAX (902) 494-6889

DATE 23 APRIL 1992

AUTHOR KEVIN JOSEPH DESROCHES

TITLE A SUBSIDENCE, COMPACTION, PRESSURE, TEMPERATURE, AND MATURITY HISTORY OF THE HIBERNIA B-08 WELL, GRAND BANKS, NEWFOUNDLAND

Degree B. SC. (HONS) Convocation SPRING Year 1992

Permission is herewith granted to Dalhousie University to circulate and to have copied for non-commercial purposes, at its discretion, the above title upon the request of individuals or institutions.

Distribution License

DalSpace requires agreement to this non-exclusive distribution license before your item can appear on DalSpace.

NON-EXCLUSIVE DISTRIBUTION LICENSE

You (the author(s) or copyright owner) grant to Dalhousie University the non-exclusive right to reproduce and distribute your submission worldwide in any medium.

You agree that Dalhousie University may, without changing the content, reformat the submission for the purpose of preservation.

You also agree that Dalhousie University may keep more than one copy of this submission for purposes of security, back-up and preservation.

You agree that the submission is your original work, and that you have the right to grant the rights contained in this license. You also agree that your submission does not, to the best of your knowledge, infringe upon anyone's copyright.

If the submission contains material for which you do not hold copyright, you agree that you have obtained the unrestricted permission of the copyright owner to grant Dalhousie University the rights required by this license, and that such third-party owned material is clearly identified and acknowledged within the text or content of the submission.

If the submission is based upon work that has been sponsored or supported by an agency or organization other than Dalhousie University, you assert that you have fulfilled any right of review or other obligations required by such contract or agreement.

Dalhousie University will clearly identify your name(s) as the author(s) or owner(s) of the submission, and will not make any alteration to the content of the files that you have submitted.

If you have questions regarding this license please contact the repository manager at dalspace@dal.ca.

Grant the distribution license by signing and dating below.

_____ _____

Name of signatory Date

Abstract

The Jeanne d'Arc basin is one of several of Late Triassic basins in Atlantic Canada, some of which contain significant quantities of hydrocarbons. The Jeanne d'Arc basin has extensive overpressuring associated with the Fortune Bay Shale. Numerical modelling of data from one well, Hibernia B-08, promotes an understanding of the nature of the overpressuring in the Hibernia field, and the timing of organic maturation of the major source unit, the Egret Member. Mathematical models of temperature, pore pressure, and hydrocarbon kinetics, applied to a series of stratigraphic columns derived by decompacting a generalized version of the present-day stratigraphy, represent the dynamics of the well site through time. Overpressure in the well does not appear to relate to rapid compaction effects, because burial history models show that subsidence and sedimentation rates have been consistently low for the last 60 Ma, placing an upper limit on the age of overpressure development. Shale transformations, which release water and are often cited as producers of overpressures, commonly occur at burial depths between 2000 and 3500 m. Rapid subsidence in the Late Jurassic and the Early Cretaceous buried much of the underlying shales below 3500 m before 60 Ma. Thus hydrocarbon generation, which began at 75 Ma, and continues today, is the source for overpressure in the area of Hibernia B-08.

KEY WORDS: Jeanne d'Arc; basin analysis; compaction; maturity; pressure; overpressure; model; heat flow

TABLE OF CONTENTS

CHAPTER 5 DISCUSSION

CHAPTER 6 CONCLUSIONS

APPENDIX A RESULTS OF SENSITIVITY ANALYSIS OF MODEL ASSUMPTIONS

TABLE OF FIGURES

TABLE OF TABLES

ABBREVIATIONS

Abbreviation	Name	Units	Remarks
c	compaction factor	none	Sclater and Christie (1980)
k	compaction factor	none	Falvey and Middleton (1981)
Φ	porosity	none (%/100)	
Φ_o	surface porosity	none (%/100)	
z	depth	m (or km, where stated)	
Q	heat flow	mW/m^2	
dT/dz	thermal gradient	°C/km	
λ	thermal conductivity	W/mK	
K	permeability	md (milli darcy)	
S_o	shape factor	none	
d_m	mean particle diameter	mm	
P	pore pressure	kPa	
S	overburden load	kPa	
σ	effective stress	kPa	
g	gravitational acceleration	m/s^2	
ρ	density	kg/m^3	

ACKNOWLEDGEMENTS

I would like to thank M. A. Williamson and D.B. Clarke, for critical reviews and encouragement. This paper benefitted greatly from conversations with A.C. Grant and P.N. Moir. I would also like to thank my fellow inhabitants of 2009, without whom none of this would have been any fun.

CHAPTER 1 INTRODUCTION

1.1 Background

Studies in petroleum geology require an understanding of the temporal and spatial occurrence of certain physical, chemical, and structural events. Some of the most important events include source rock maturity, primary and secondary migration, cap rock and reservoir porosity, and permeability reduction with compaction and diagenesis. These temporal features are the products of the interaction of physical, chemical, and geologic processes; their numerical simulation is, therefore, a multi-disciplinary task.

Techniques developed by Perrier and Quiblier (1974), Stecklar and Watts (1978), and van Hinte (1978) permit quantitative estimation of subsidence history, sedimentation rate, and changes in stratigraphic thickness through time at any point in basin. The integration of these techniques with models of hydrocarbon reaction kinetics, pressure, and thermal history (Mudford and Best 1989; Sweeney and Burnham 1989; Sweeney et al. 1987; Ungerer et al. 1990) make possible the reconstruction of the conditions that prevailed throughout the history of a basin. Such a framework will allow, in some circumstances, the prediction of the timing of important events in the hydrocarbon generation history of a basin.

1.2 Objective and Scope

Williamson (in press) analyzed the maturation and thermal history of the source interval for the Jeanne d'Arc basin, Grand Banks, Newfoundland (Fig. 1.1). He demonstrated that the source unit, the Egret Member of the Rankin Formation (Fig. 1.2), began producing hydrocarbons

in the region of the Hibernia oil field approximately 60 my ago. The objective of this study is to present a detailed analysis of the compaction history, pressure generation, temperature development, and maturation history for the Hibernia B-08 well (Fig. 1.1).

This analysis is limited to one well for several reasons. Many basin modelling techniques analyze the data in a well-by-well manner, correlating and interpolating the results between wells (Ungerer et al. 1990; Williamson in press). A detailed analysis of one well, particularly with respect to the sensitivity of the model to variability in assumptions, will help to constrain larger scale studies. Also, it allows detailed modelling of pressure effects, which are important locally and often vary regionally. The B-08 well was chosen from the Hibernia field because of the combination of its good biostratigraphic, litholologic, vitrinite reflectance, and pressure data.

One limitation of a single well analysis is that wells are often drilled on structural highs and so results may not be easily extrapolated to the surrounding area. This is the case with Hibernia B-08. Therefore, to analyze an entire basin, many wells, integrated with seismic data, should be modelled. Such a comprehensive survey is beyond the scope of this study.

1.3 Geology of the Grand Banks

1.3.1 Introduction

Attempts to model hydrocarbon distribution must consider tectonic history, basin structure, and sedimentation patterns as they influence pressure and temperature development in a basin. This section provides a brief overview of the structure, stratigraphy, and tectonic history of the Grand Banks.

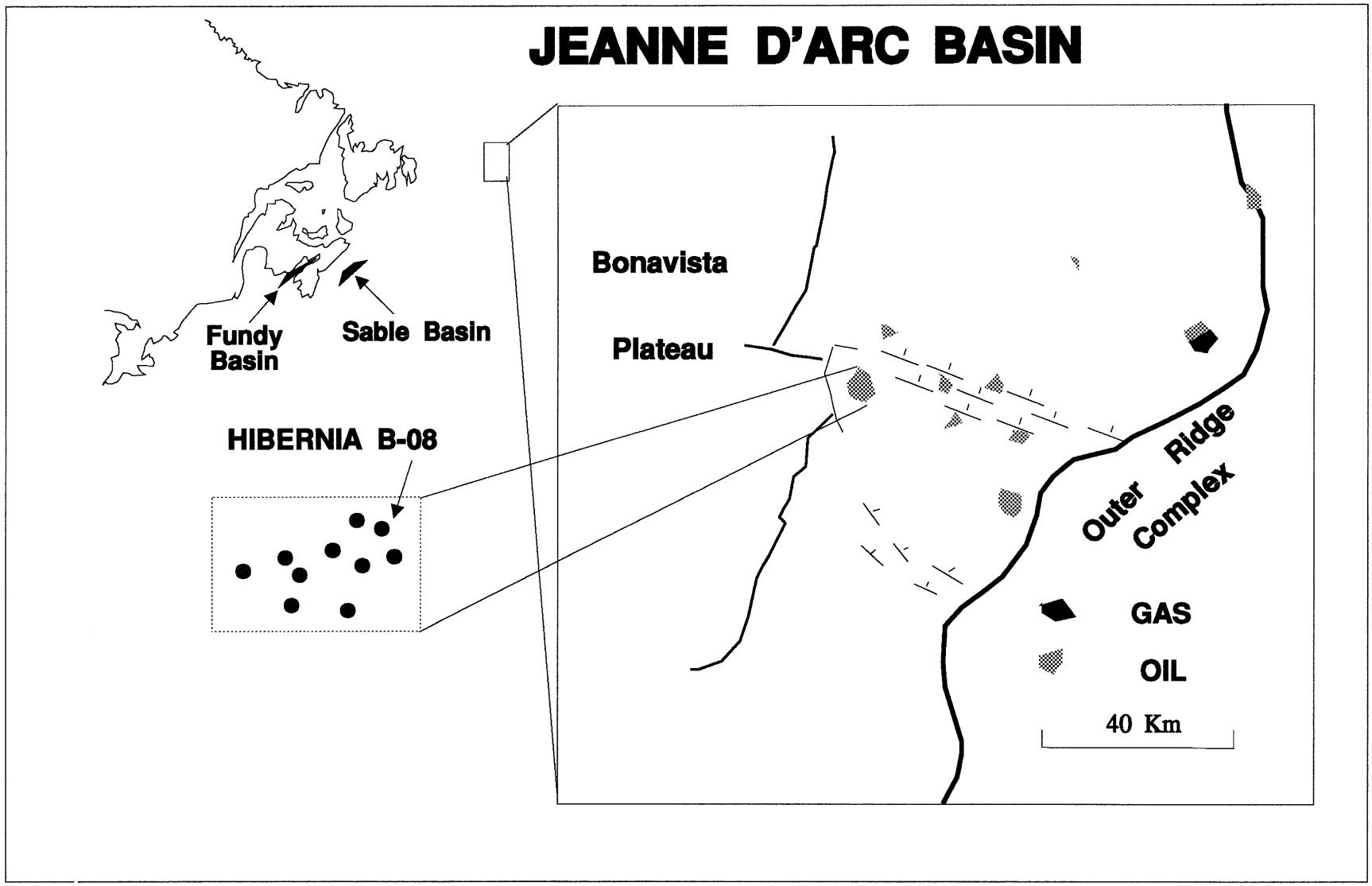

Figure 1.1 Location of study area.

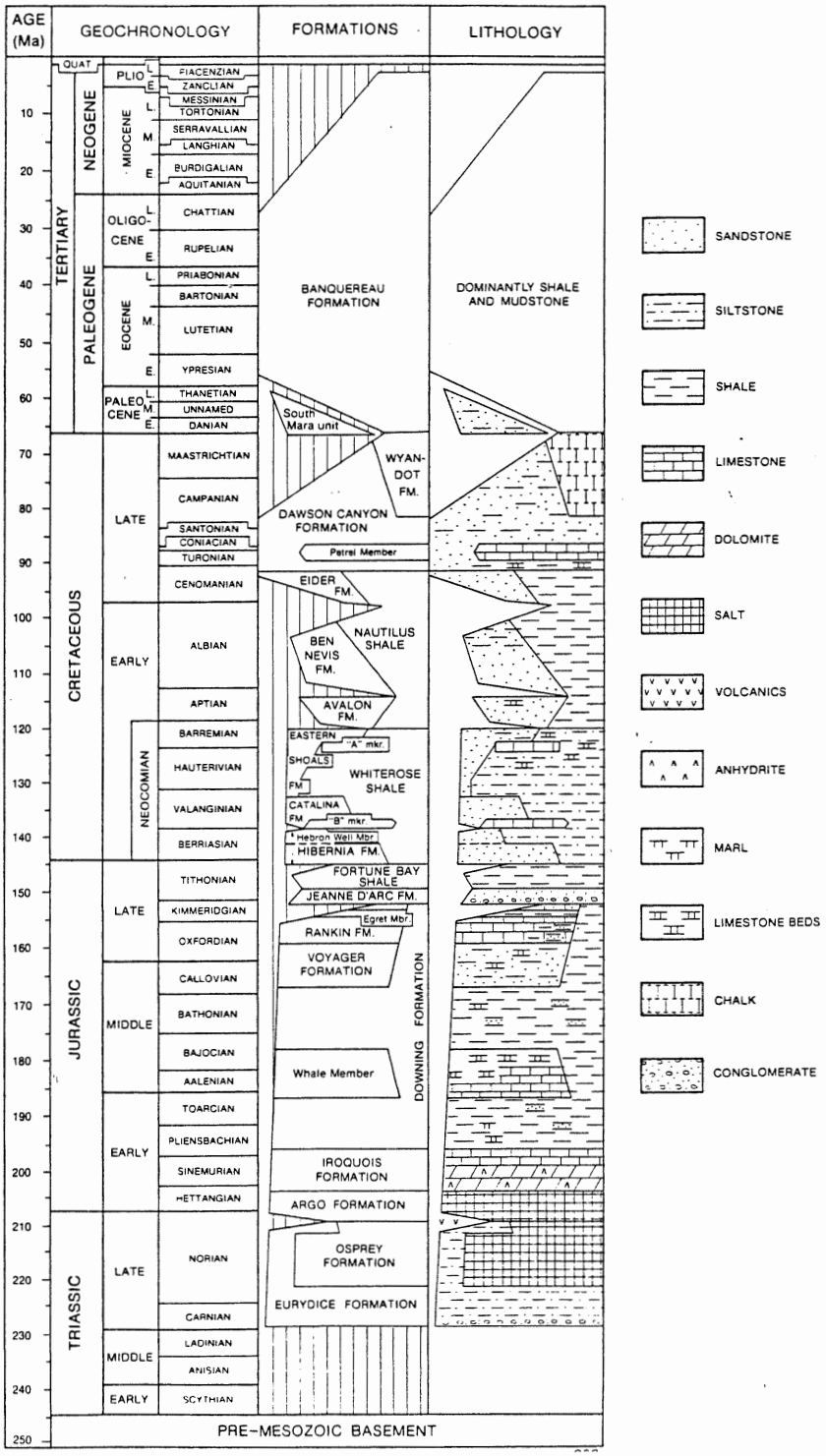

Figure 1.2 Stratigraphy of the Grand Banks (McAlpine 1990).

1.3.2 Physiography of the Grand Banks

A series of interconnected Mesozoic basins underlie the Grand Banks (Grant et al. 1986). These are the Whale, Horseshoe, and South Whale basins in the south, the Jeanne d'Arc, Carson, and Flemish Pass basins in the central Grand Banks, and the East Newfoundland basin in the north (Fig. 1.1). The Jeanne d'Arc basin is of particular economic interest because of its proven hydrocarbon reserves and potential.

The Jeanne d'Arc basin is a fault-bounded half graben (deVoogd and Keen 1987), flanked to the west by the Bonavista Platform and to the east by the Outer Ridge Complex (Fig. 1.1) (Grant et al. 1986). It is the deepest of the Grand Banks basins and provides the most complete stratigraphic record of Grand Banks evolution (Grant and McAlpine 1990). Sediment thickness increases from 4 km in the south to greater than 20 km in the north (deVoogd and Keen 1987).

1.3.3 Evolution of the Jeanne d'Arc basin

Late Triassic rifting of eastern Canada created a series of northeast-trending grabens that include, among others, the Fundy, Sable and Jeanne d'Arc basins (Fig. 1.1). These grabens became the depocenters for thick sequences of terrestrial red beds and evaporites (Grant et al. 1986). Rifting that eventually led to the creation of the North Atlantic Ocean proceeded from south to north, beginning in the Early Jurassic along the Scotian margin. Transform motion along the Newfoundland Fracture Zone, which forms the southern edge of the Grand Banks, accommodated this extension (Grant et al. 1986 and Tankard and Welsink 1987). Thermal uplift and peneplanation of the southern Grand Banks, known as the Avalon Uplift, preceded rifting of the Grand Banks margin which began in the Kimmeridgian (Grant et al. 1986) or the Callovian

(Tankard and Welsink 1988). Rifting of the margin was complete by the Paleocene (Grant et al. 1986; Grant and McAlpine 1990).

The effect of this complex tectonic history on the structure of the basin is difficult to decipher because of the effects of salt diapirism. Grant and McAlpine (1990) consider much of the faulting within the sediments to be related to salt movement. Enechescu (1987) and Tankard and Welsink (1987) consider transform fault motion to play a dominant role, however they differ on the location of the controlling transform faults. As diapirism does not appear to be important in the Hibernia area, its effects are not considered in this study.

1.4 Pore pressure

Much of this study deals with the development of models to describe the pressure regime of the Hibernia B-08 well. The purpose of this section is to outline a few terms and concepts that are important to an understanding of pressure development in a sedimentary column.

Hydrostatic pressure is the pressure exerted by the weight of overlying pore fluid. Under equilibrium pressure conditions, fluid pressures will be hydrostatic. The *lithostatic pressure* refers to the pressure at which the grain matrix is totally supported by the pore fluid. This is the maximum pressure that a pore fluid can exert; pressuring to this level results in the grains floating unstably in the pore fluid (Fertl 1976).

The *hydrostatic gradient* and *lithostatic gradient* are graphical representations of the hydrostatic and lithostatic pressures (Fig. 5.1). Pressures between these two gradients, *overpressures*, occur when pore fluids support part of the weight of the grain matrix as well as that of the overlying fluid.

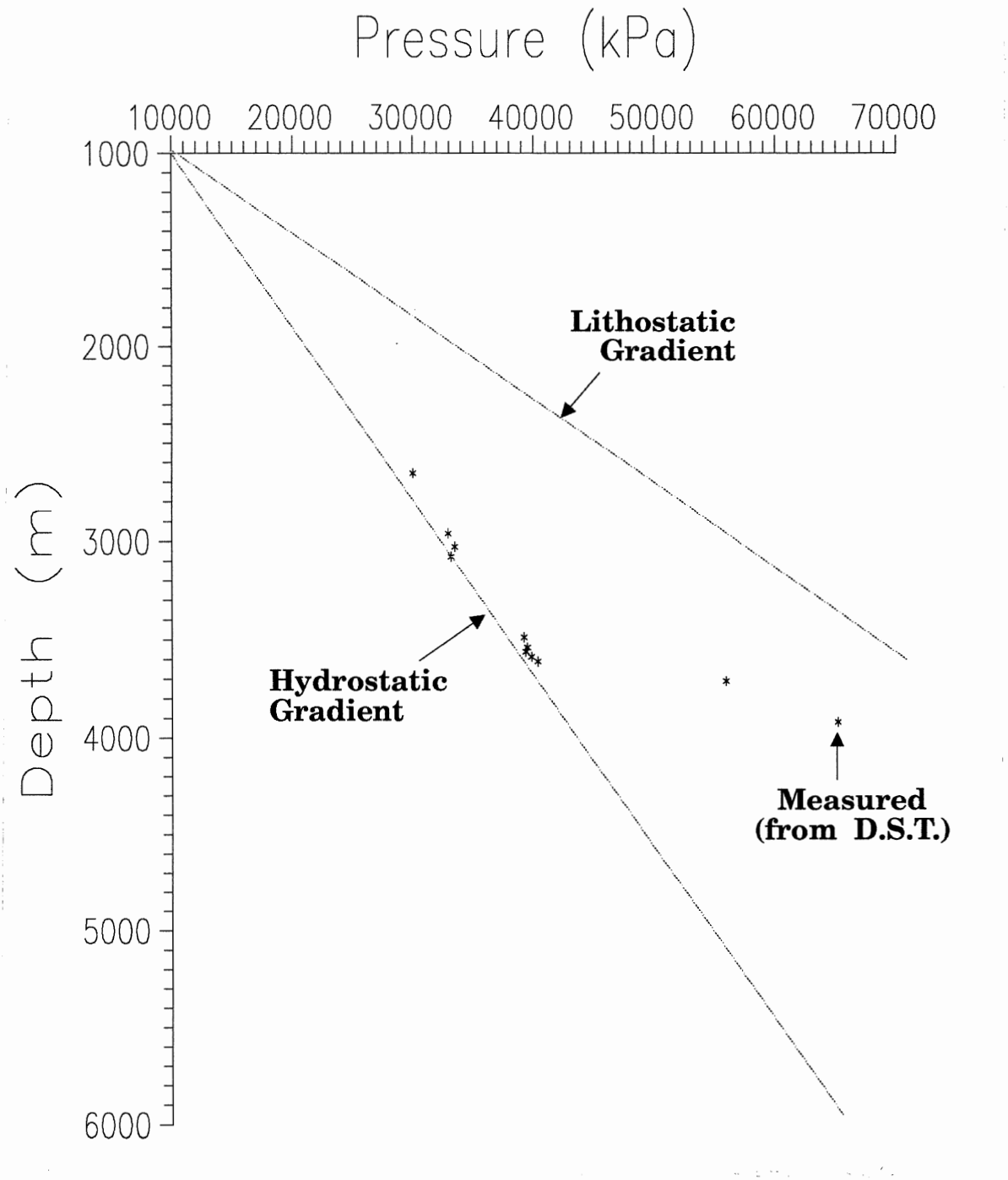

Figure 1.3 A typical porosity-depth diagram, outlining the pressure gradients and the zone of overpressuring. See Section 1.4 for definitions.

1.5 Organization

For readers unfamiliar with the various modelling techniques applied in this study, Chapter 2 serves as an outline of the mathematical concepts, limitations, and assumptions that are important in basin modelling. Chapter 3 outlines the sources of the data used in this study, and describes how the data fits into the modelling scheme. Chapters 4 and 5 present and discuss the model results, respectively. Appendix A provides a study of the sensitivity of the models to variability or uncertainty in important physical and mathematical parameters.

CHAPTER 2 BASIN MODELLING

2.1 Analytical Techniques

2.1.1 Introduction

There exist a variety of techniques to investigate the depositional and chemical history of a sedimentary basin (Nakayama and Van Siclen 1981; Keen and Beaumont 1990; Ungerer et al. 1990). The usefulness of these techniques is their ability to integrate pressure, temperature, maturity, and hydrocarbon generation models. The main modelling tool used in this study is the BasinMod software package from Platte River Associates. BasinMod incorporates the algorithms of Sweeney et al. (1987), Ungerer et al. (1990), and others. This section is a brief discussion of these algorithms, together with their assumptions and limitations.

2.1.2 Decompaction

Decompaction is a technique developed by Perrier and Quiblier (1974) and Stecklar and Watts (1976) that recovers the original thickness of a sedimentary unit at the time of its deposition. This technique allows more accurate calculation of changes in sedimentation rate through time, and enables better reconstruction of past physical conditions in the basin.

The technique uses a model which defines the volume of the sedimentary column as the sum of the volume of grains and the volume of pores. The model is one dimensional, meaning any change in volume is due solely to changes in the vertical thickness of the sedimentary column. Assuming the grain volume is constant, the decrease in thickness of a stratigraphic unit during burial results from porosity loss. Thus, recovering the pre-compaction thickness of the sedimentary

unit becomes a matter of adding the porosity lost during burial.

The assumption that grain volume remains constant through time is invalid in cases where dissolution and cementation occur. These cases include marls and some carbonates, however, for most clastic deposition the approximation should be reasonable (Sclater and Christie 1980).

Division of the stratigraphic column into horizontal layers of known age precedes decompaction. For brevity, depths of known age will be referred to as *age-depth pairs*. This study uses biostratigraphic and seismic data to define these parameters.

Figure 2.1 is a graphical representation of the decompaction process. The uppermost layer (A), bounded above by the present-day depositional surface, z(0), and below by z(1) (which represents a time in the past t(1)), is removed. The upper boundary of layer B, z(1), rises to become the depositional surface, z'(1), and the remaining layers thicken in response to the decreased load, creating the new boundaries z'(2), z'(3), and so on. The column now represents the sedimentary column at time t(1). In a similar manner, the procedure is repeated for the intervals representing times t(2), t(3), etc.

Because compaction results in porosity loss, the amount of thickening that occurs in each unit during decompaction is a result of recovered porosity. To calculate the change in porosity that occurs when a unit changes depth, a porosity-depth function is derived. Sclater and Christie (1980) defined the porosity-depth function as an exponential:

$$\Phi=\Phi_o e^{-cz} \qquad \text{Eqn 2.1}$$

where Φ is fractional porosity, Φ_o is surface porosity, c is a lithology-dependent constant, and z is depth (in km). Falvey and Middleton (1981) however, applied an inverse relationship to porosity:

$$\frac{1}{\Phi} = \frac{1}{\Phi_o} + kz \qquad \text{Eqn 2.2}$$

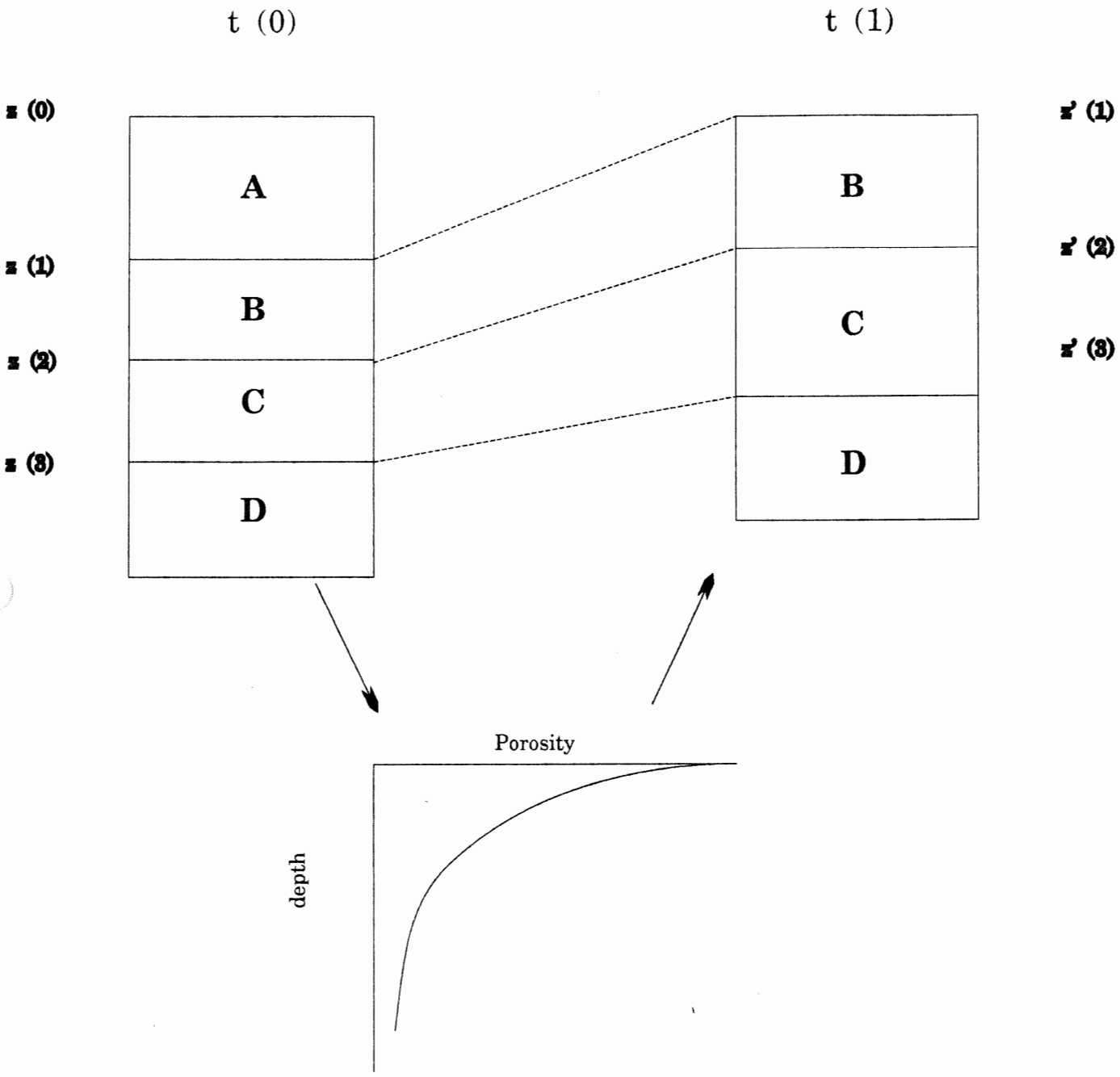

Figure 2.1 This is a graphical illustration of the decompaction procedure. Removing unit A from the column t(0) results in thickening of the units beneath. This thickening is the result of increased porosity, resulting from reduced overburden load. The volume of porosity returned to the units is quantified by the porosity-depth curve. See text for discussion.

where k is a different lithology-dependent function.

This study employs the exponential function (Eqn. 2.1), as it better reproduces observed porosity (from calculations using sonic transit time). Figure 2.2 compares the shape of different porosity functions with data from Hibernia B-08. The sensitivity analysis, summarized in Appendix A, includes a result of a comparison of the decompaction techniques using data from this study.

2.1.3 Thermal modelling

The thermal history of sediments and fluids within a sedimentary column governs source rock maturation and petroleum generation. Modelling this thermal history is, therefore, an important element in the analysis of the hydrocarbon potential of a basin.

This study considers the sedimentary column as a series of stacked horizontal layers, heated from below (Ungerer et al. 1990). Each layer corresponds with lithologic units defined by age-depth pairs. The method is useful for two reasons. First, unique thermal parameters define each layer. This is important because porosity and thermal conductivity, factors which control heat transport through a rock unit, depend on lithology. Also, by selecting layers that coincide with the age-depth pairs used to decompact the sedimentary column, the thermal structure of the basin can be calculated at each decompaction step.

The models assume that each layer maintains thermal equilibrium (Waples et al. 1992a). This means that heat flowing into the bottom of the unit matches the heat flowing out of the top. Therefore, there is no contribution of heat from radiogenic sources within the layer, no gain or loss of heat through lateral fluid movement, and no loss of heat to pore fluid convection. Lateral

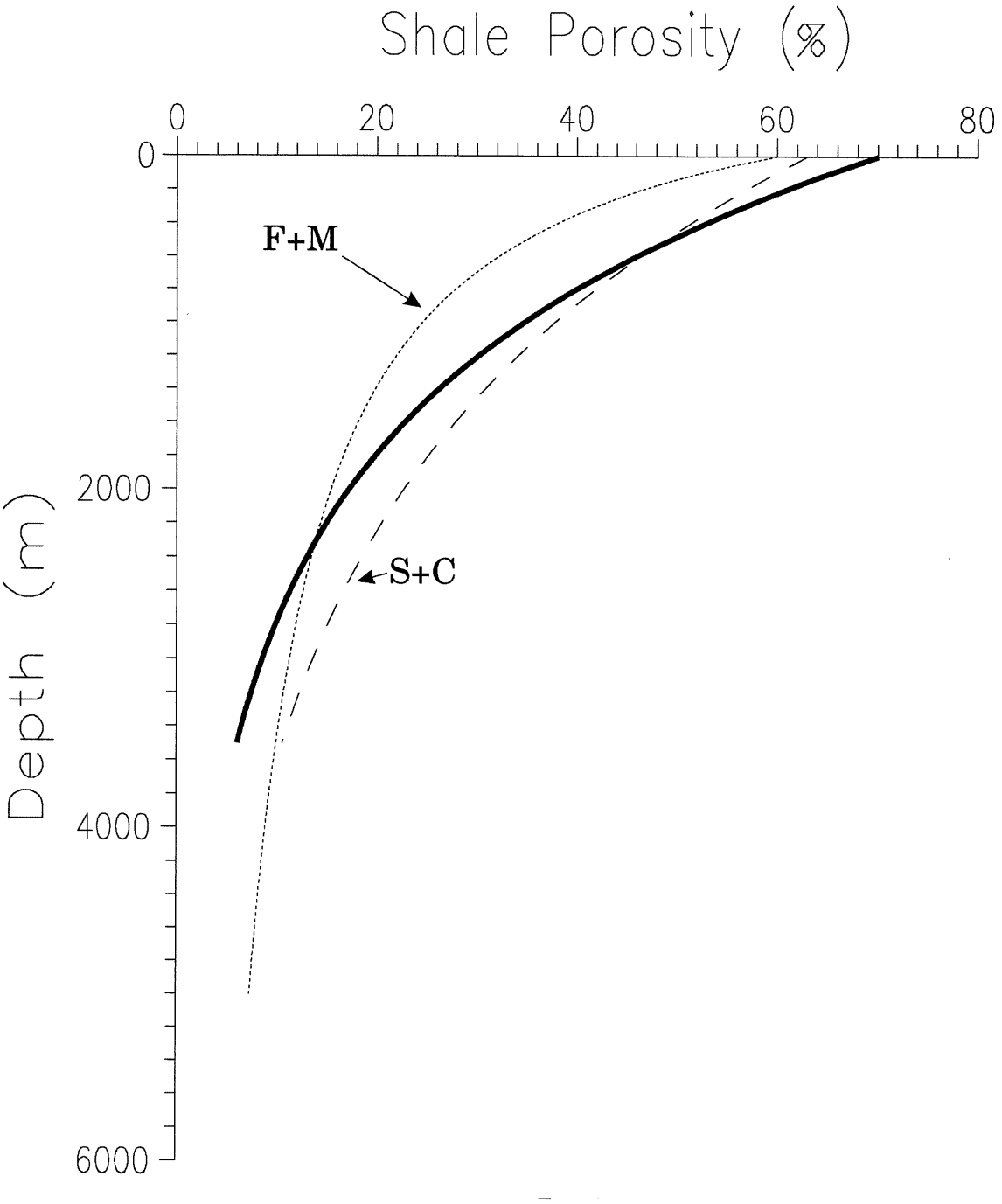

Figure 2.2 Several examples of shale porosity-depth functions. The curve marked S+C represents that of Sclater and Christie (1980) and F+M, Falvey and Middleton (1981). The bold curve, described by Sclater and Christie (1980) parameters, is the function adopted in this study.

fluid flow may be important near the margin of a basin, in faulted strata, and near piercement structures (Mudford and Best 1989). Also not considered in the model are local convection effects, including compaction-driven circulation (Cathles and Smith 1983) and free-convection, resulting from the thermal expansion of pore water (Combarnous and Bories 1975). These limitations preclude a complete picture of the thermal behaviour of the sedimentary column on a fine scale; despite this, the models are useful for modelling basin-scale thermal features (Waples et al. 1992a, b; Williamson in press).

Thermal conductivity varies with temperature, porosity, matrix conductivity, pore fluid content, and confining pressure (Huang and Williamson, in preparation). The thermal model considered here takes into account the effects of porosity, temperature, and matrix conductivity, but not pressure. All pore fluids in the model are considered to have the same thermal conductivity values as sea water. These limitations are valid for large scale thermal modelling, because the effects of confining pressure and pore fluid changes should be small (Correia et al. 1990).

Heat flow through the stratigraphic column (Q) is calculated as the product of geothermal gradient (dT/dZ) and bulk thermal conductivity (λ) (Correia et al. 1990; Ungerer et al. 1990; Waples et al. 1992a):

$$Q=\lambda \cdot dT/dZ \qquad \text{Eqn 2.3}$$

Corrected bottom hole temperatures (BHT's) constrain the geothermal gradient. Temperature and porosity corrections applied to the thermal conductivity values of the grains create values for use in Equation 2.3.

Porosity corrections are made by applying the following relationship (Ungerer et al. 1990):

$$\lambda_{eff} = [\lambda_g \cdot (1-\Phi)] \cdot [\lambda_w \cdot \Phi] \qquad \text{Eqn 2.4}$$

where λ_{eff}, λ_g, and λ_w are the effective, grain, and pore water conductivities respectively. The effective thermal conductivity (λ_T), is then corrected for temperature (Waples et al. 1992a):

$$\lambda_T = \frac{\lambda(0)}{(1+aT)} \qquad \text{Eqn 2.5}$$

where $\lambda(0)$ is the thermal conductivity at 0°C, T is the temperature, and a is an empirically derived constant.

2.1.4 Permeability and pore pressure

The most commonly used theoretical approach to calculating permeability in porous media is the Kozeny-Carmen equation (Bear 1972). This model considers the porous media as a series of parallel conductive tubes of equal length. The original equation determines permeability (K) in terms of effective porosity (Φ'), the porosity available for fluid flow; and shape factor (S_o), a measure of grain surface area per volume (in m^2/m^3):

$$K = \frac{\Phi'^3}{5S_o(1-\Phi')^2} \qquad \text{Eqn 2.6}$$

The shape factor is related empirically to mean particle diameter by the relationship (Bear 1972):

$$d_m = \frac{6}{S_o} \qquad \text{Eqn 2.7}$$

Combining these equations relates permeability and grain size:

$$K = \frac{d_m}{S_o} \frac{\Phi'^3}{(1-\Phi')^2} \qquad \text{Eqn 2.8}$$

These equations adequately describe the permeability-porosity relationship for sandstones, but not for the extremely low permeabilities found in highly compacted shales (Ungerer et al.

1990). As a consequence, this study adopts a modified version of Equation 2.8 for lithologies having porosity less than 10 % (Ungerer et al. 1990):

$$K=\frac{20}{S_o}\frac{\Phi'^3}{(1-\Phi')^2} \qquad \text{Eqn 2.9}$$

or, using average grain size:

$$K=\frac{5d_m}{9}\frac{\Phi'^5}{(1-\Phi')^2} \qquad \text{Eqn 2.10}$$

The porosity-depth function described earlier determines the porosity values used to calculate permeability. Predictions of porosity from sonic travel time logs serve as constraints for the porosity-depth function.

This study applies default grain size parameters to these equations. Accurate measurements of grain size are not common in offshore wells due to the expense of coring. A few grain size measurements made on frequently cored reservoir rocks would not accurately describe the grain size throughout the well, therefore, using textbook estimates is the simplest way of excluding bias from the model. The sensitivity analysis, summarized in the appendix, discusses the effects of uncertainty of this parameter on the pressure, porosity, and permeability models generated in this study.

Pore pressure is calculated using the method of Smith (1971), in which the pore pressure (P) is related to the vertical stress on the grain-grain contacts (S) and the effective stress (σ):

$$\sigma=S-P \qquad \text{Eqn 2.11}$$

The vertical stress is defined as the loading pressure of overlying sediment and water:

$$S=\rho_b \cdot gz \qquad \text{Eqn 2.12}$$

where ρ_b is the mean bulk density of overlying strata and pore fluids, g is the acceleration due to

gravity, and z is burial depth.

The model considers the effects of compaction on porosity loss and fluid pressure, however it omits the effects of pressure dissolution and high geothermal gradients (Smith 1971; Ungerer et al. 1990). Other factors not considered, but important in the development of overpressures, are hydrocarbon generation, fluid release resulting from clay mineral transformations, and thermal expansion of water (Sclater and Christie 1980; Ungerer et al. 1990). Section 5.5 contains a more detailed discussion of the importance of these factors with respect to the pressure regime in the Hibernia field.

2.1.5 Hydrocarbon kinetics

The main goal of petroleum geology investigations is a greater knowledge of the hydrocarbon distribution in the target basin. To this end, several physical/chemical models describe the progressive maturation of source rocks and the production of hydrocarbon fluids.

Earlier generation chemical models assigned reaction rates with respect to temperature and time, but did not consider the heterogeneous chemistry that typifies most hydrocarbon source rocks (Waples 1980). Recent studies have produced models which can account for multiple, simultaneous reactions within the source interval (Burnham and Sweeney 1989; Tissot et al. 1987).

This study uses the VITRIMAT method of Burnham and Sweeney (1989) to predict source rock maturation in terms of vitrinite reflectance. This method uses the Arrhenius equation to model the maturation of kerogen:

$$k=Ae^{(-E/RT)} \qquad \text{Eqn 2.13}$$

where R is the ideal gas constant, T is temperature (K), and k, A, and E are the rate constant,

frequency factor, and activation energy, respectively, for each chemical reaction. The latter three variables uniquely define any first order reaction.

The VITRIMAT method calculates the reaction rate based on a series of reactions, each defined by Equation 2.13. Each reaction occurring in the maturing kerogen, for example, the production of water, carbon dioxide, methane, and higher hydrocarbons, is represented by unique rate constants, frequency factors, and activation energies. Type II kerogen parameters define the Egret Member (Snowden and Fowler 1986). Type II hydrocarbons are generally marine, oil-prone sources (Grant et al. 1986). Discussions by Burnham and Sweeney (1989) and Sweeney et al. (1990) deal with the derivation and conversion of this expression into vitrinite reflectance units.

2.2 Modelling procedure

Modelling basin development and hydrocarbon history involves integrating the physical and chemical models outlined above into one, or several, geological models. In practice the computer allows all the models to run essentially simultaneously, but in theory the procedure is sequential. This section outlines this procedure.

The first step is to perform a sensitivity analysis of model assumptions. The goal of this is to constrain physical and geological assumptions using measured data. An example is the use of sonic transit time to constrain porosity-depth functions. Other important parameters that also must be constrained are heat flow, thermal conductivity, grain size, and kerogen type. Appendix A discusses the sensitivity analysis performed for this study.

Because Equation 2.3 relates thermal conductivity and heat flow, constraining either one requires some external constraint on the other. Constraint may take the form of measured thermal

conductivities or a geophysical model that determines heat flow. Many rift models predict heat flow (Keen and Beaumont 1990) and are useful for this purpose. Measured thermal conductivity values from the Jeanne d'Arc basin (Correia et al. 1990) provide constraints for this study.

Decompaction of the generalized stratigraphic column proceeds after selection of the basic parameters. The result is a burial history curve which plots the change in thickness and burial depth of units through time. The next step is to calculate permeability, pressure, temperature, and organic maturity models. The result is a comprehensive physical model, which, when integrated with hydrocarbon kinetic techniques produces a petroleum generation model.

CHAPTER 3 DATA

3.1 Introduction

Hydrocarbon modelling requires the integration of data from a variety of geoscience disciplines. Models developed in this study incorporate paleontological, lithological, thermal, geochemical, geophysical, pressure, and sonic log data. This chapter is a survey of the sources and uses of the data collected for this study.

3.2 Biostratigraphy

Table 3.1 summarizes the biostratigraphic data used in this study as a series of depths and corresponding ages (Ascoli 1983 and 1988). Seismic extrapolation (Williamson in press) of paleontologic horizons from neighbouring wells permits extension of the age-depth pairs to below the total depth of the well.

The age-depth pairs enable partitioning of the sedimentary column into layers for decompaction. Owing to the distribution of paleontological data in the well, the stratigraphic packages used in the decompaction sometimes do not correlate exactly with lithostratigraphic boundaries. Figure 3.1 demonstrates this by comparing the stratigraphy used in the model with that of McAlpine (1990).

3.3 Lithology

Lithology logs, based on interpretations of gamma and sonic logs, provide the lithologic information used in this study (Canadian Stratigraphic Services Ltd. 1982). The lithology is

Depth (m)	Age (Ma)	Comments
300	10	
600	23	
900	36	
1200	50	
1500	63	
1741	65	
1741	75	Hiatus
2052	86	
2113	88	
2113	90	Hiatus
2145	104	
2145	114	Hiatus
2164	116	
2491	122	
2521	123	
2915	130	
3155	135	
3176	135.5	
3475	137	
3650	145	
3848	147	
4500	150	seismic
5185	153	seismic
5285	155	seismic
5585	160	seismic

Table 3.1. Depths and corresponding ages for Hibernia B-08. All depths from paleontological data (Ascoli 1988) except where marked 'seismic', which are from seismic interpretations and correlation from other wells (Williamson 1992). Depths repeated in the table represent hiatuses; the corresponding ages refer to the beginning and end of the hiatus.

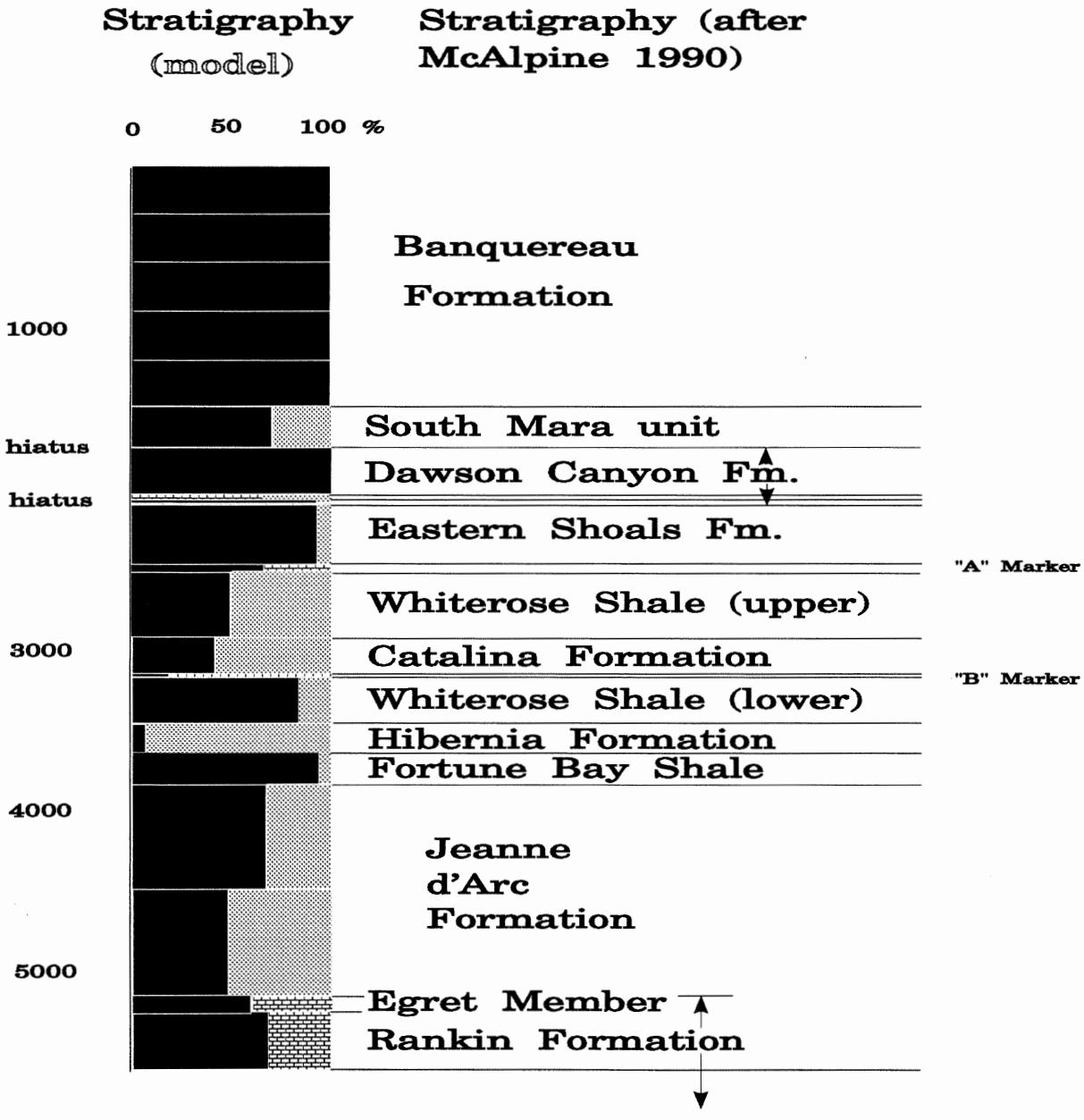

Figure 3.1 Stratigraphic model based on age-depth pairs (see text) for Hibernia B-08, and lithology (Canadian Stratigraphic Services Ltd. 1982) and the stratigraphy of McAlpine (1990).

entered into the model as a sandstone/shale/limestone ratio for each layer defined by the age-depth pairs. Thus a layer which in reality is a series of interlaminated sand and shale beds may become an homogeneous layer of 50% sand and 50% shale. Table 3.2 and Fig. 3.1 summarize the lithologic generalization used in the model.

3.4 Thermal data

Thermal data (Table 3.3) used in this study include corrected bottom hole temperature measurements made during logging runs (Moir and Whidden 1989), and measurements of the matrix thermal conductivity. This study considers two sets of matrix conductivity values (Table 3.4): Set 1, measured and assumed values from a previous study of the Jeanne d'Arc basin (Correia et al. 1989), and Set 2, based on laboratory measurements from Scotian Shelf sediments (Keen and Lewis 1982). The models presented here use Set 1; Appendix A-2 shows the differences in modelling results using Set 2 values.

3.5 Vitrinite reflectance

Vitrinite reflectance is a measure of the organic maturity of sediments. In this study, vitrinite reflectance helps constrain modelled thermal conductivity and heat flow parameters. Table 3.5 is a summary of reflectance measurements used in this study (Avery et al. 1986).

Unit*	Unit Top (m)	Unit Bottom (m)	Lithology
1	0	300	Shale
2	300	600	Shale
3	600	900	Shale
4	900	1200	Shale
5	1200	1500	Shale
6	1500	1741	70% Sh/ 30% Ss
8	1741	2052	Shale
9	2052	2113	60% Ls/ 40% Sh
10	2113	2145	90% Sh/ 10% Ss
12	2145	2164	Sandstone
14	2164	2491	90% Sh/ 10% Ss
15	2491	2521	60% Sh/ 40% Ls
16	2521	2915	50% Ss/ 50% Sh
17	2915	3155	60% Ss/ 40% Sh
18	3155	3176	80% Ls/ 20% Sh
19	3176	3475	80% Sh/ 20% Ss
20	3475	3650	90% Ss/ 10% Sh
21	3650	3848	90% Sh/ 10% Ss
22	3848	4500	70% Sh/ 30% Ss
23	4500	5185	60% Sh/ 40% Ls
Egret Member	5185	5285	60% Sh/ 40% Ls
25	5285	5585	70% Sh/ 30% Ls

Table 3.2. Generalized lithology used in the model of Hibernia B-08.
* - missing numbers represent hiatuses.

Table 3.3 Measured borehole temperatures (corrected BHT's) for Hibernia B-08

Depth	Temperature (oC)
1000	29.7
2000	55.4
3000	81.1
4000	106.8

Table 3.4 Thermal conductivity values used in this study.

THERMAL CONDUCTIVITY SET 1 (from Correia et al. 1990)

Lithology	Thermal Conductivity (W/m°C)
Sandstone	4.19
Shale	2.3
Limestone	2.41

THERMAL CONDUCTIVITY SET 2 (from Keen and Lewis 1982)

Lithology	Thermal Conductivity (W/m°C)
Cenozoic sand/shale	2.48
Jurassic/Cretaceous sandstone	2.2
Jurassic/Cretaceous shale	1.55

Depth (m)	Reflectance (%R_o)	error
1185	.32	.02
1275	.39	.05
1550	.42	.04
1990	.40	.04
2659	.41	.06
2669	.46	.05
2673	.47	.05
2675	.56	.05
3481	.31	.04
3482	.47	.03
3483	.47	.03
3488	.48	.05
3496	.48	.03
3554	.50	.03
3556	.47	.05
3557	.49	.03
3559	.48	.06
3562	.50	.03
3606	.54	.03
3618	.46	.04
3995	.61	.04
4115	.64	.06
4160	.64	.06
4190	.62	.09
4250	.68	.07
4340	.69	.04
4430	.61	.05

Table 3.5 Vitrinite reflectance measurements from Hibernia B-08 (Avery et al. 1986).

3.6 Pressure

Table 3.6 is a summary of pressure values generated from drill stem test results. Figure 3.2 is a plot of pressure versus depth. The top of the overpressure zone appears as a departure from the hydrostatic at approximately 3600m.

3.7 Sonic Log

Figure 3.3 is a plot of sonic transit time for the Hibernia B-08 well. Sonic transit time is sensitive to the volume of fluid-filled porosity, and is commonly used in basin studies as a porosity indicator (Keen and Beaumont 1990). Empirical methods by Magara (1976) and Schlumberger (1979) enable calculation of sandstone and shale porosity, respectively.

Figure 3.4 is a plot of shale porosity versus depth, derived from sonic transit time data. The solid line in the graph represents the mathematical function used to generalize the effects of depth on porosity. The porosity-depth functions represented by these plots are those used in the decompaction procedure described in Section 2.1.2. Literature values describe limestone porosity.

Depth (m)	Pressure
2655	29971
2959	32900
3026	33438
3076	33144
3487	39200
3538	39480
3560	39432
3580	39800
3609	40326
3710	55903
3918	65204

Table 3.6 Pressure measurements from drill stem test results.

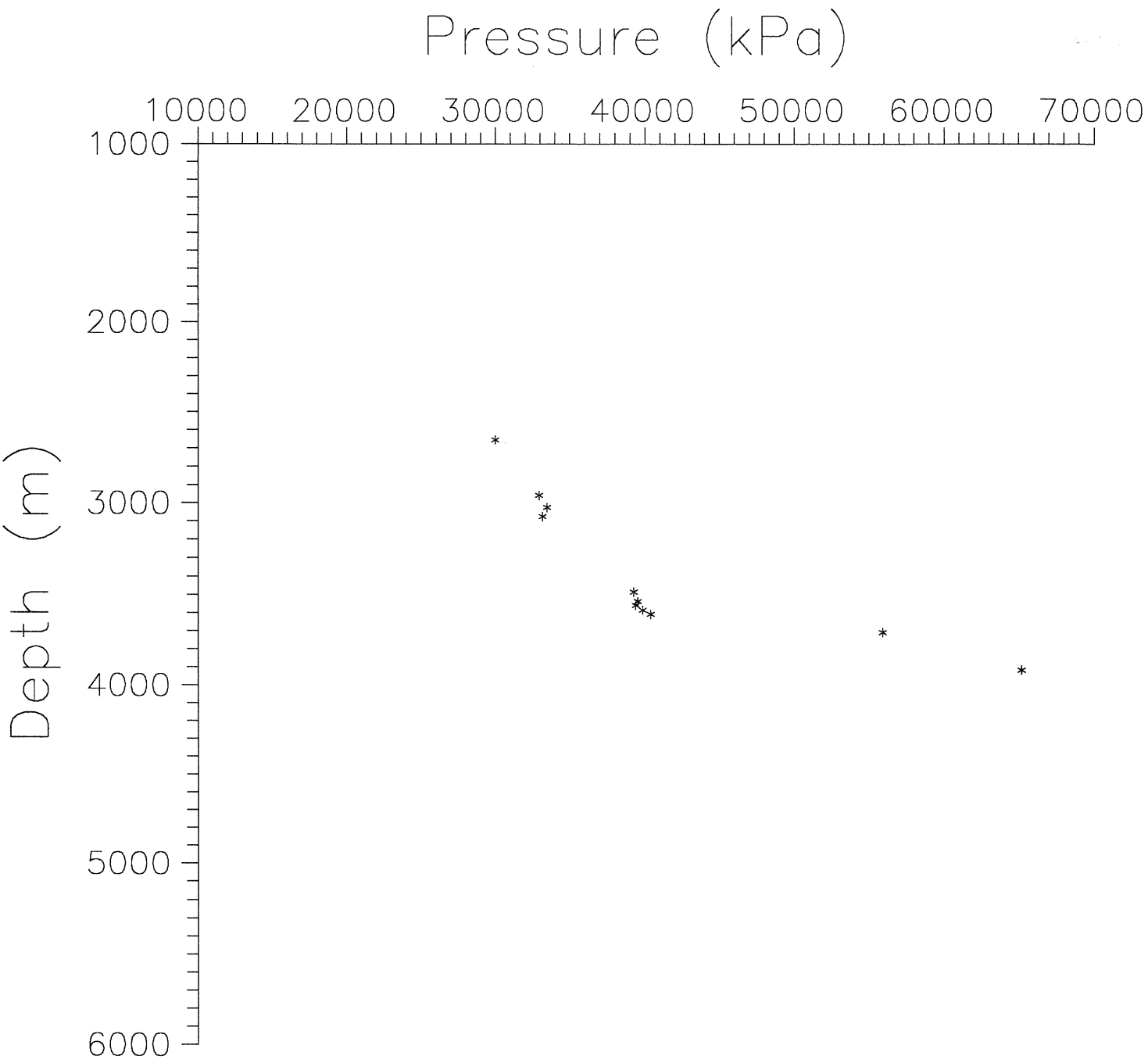

Figure 3.2 Plot of pressure values from Table 3.6 plotted versus depth. The overpressure appears as an increase in pressure at 3600 m.

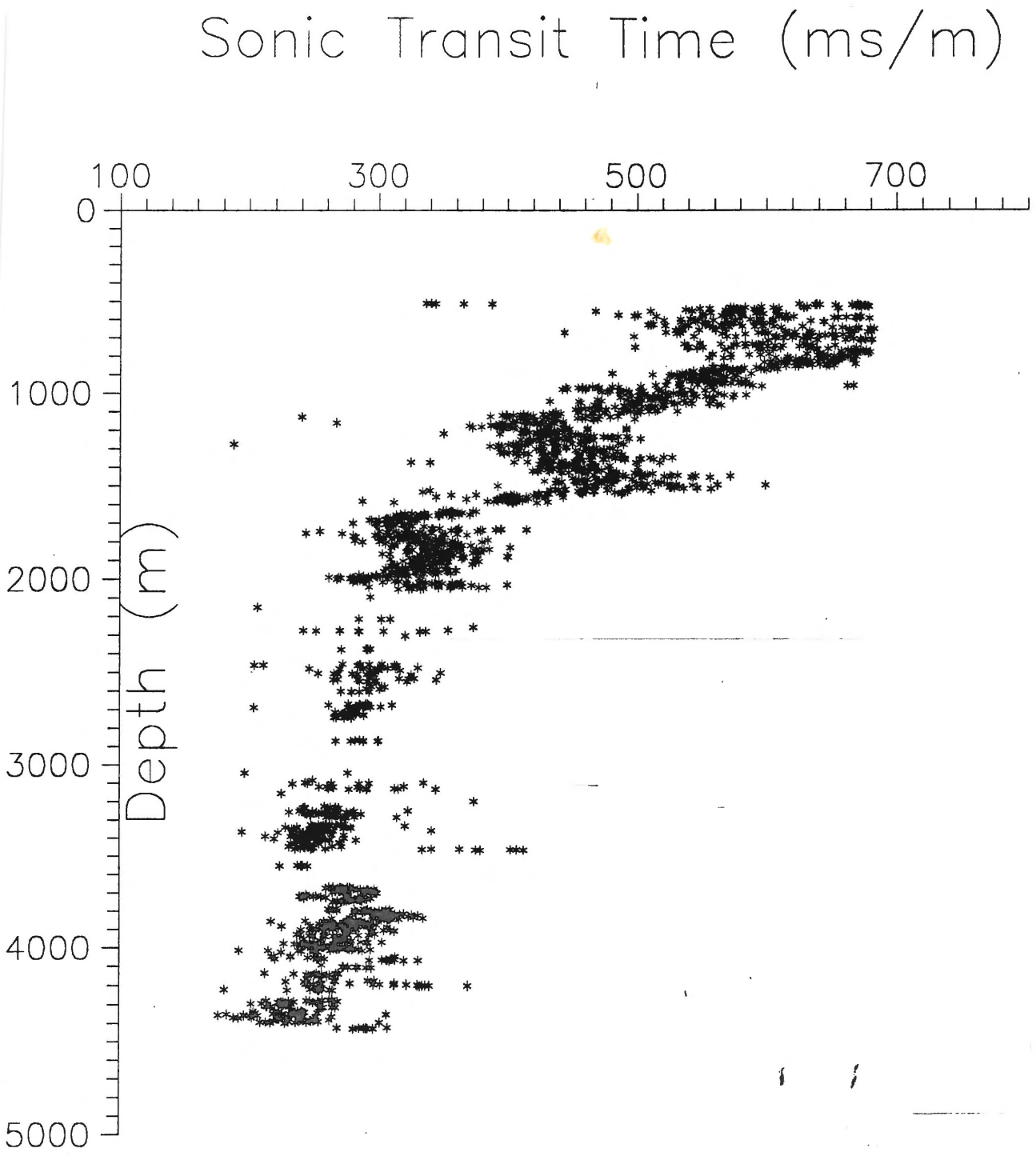

Figure 3.3 Sonic transit time. Lithology and porosity control sonic velocity. The discontinuity at 3600 m represents the zone of high porosity maintained by the overpressure.

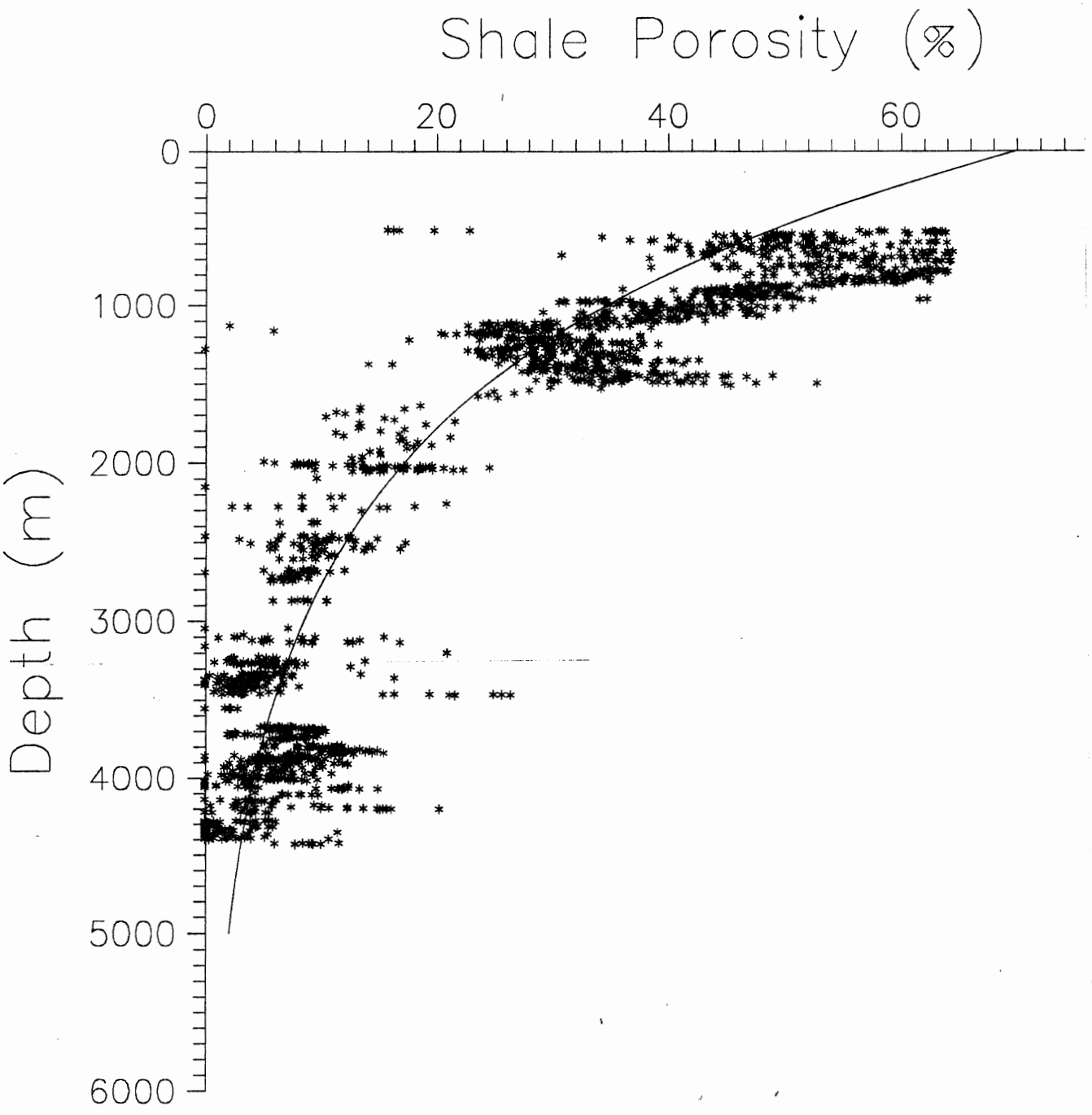

Figure 3.4 Plot of shale porosity versus depth. The porosity values are calculated from sonic transit times using the method of Magara (1976). Superimposed on the data is the porosity-depth function used in this study. The curve corresponds to Eqn. 2.1 with c= 0.70 and Φ_o= 0.70.

3.8 Summary

Age-depth pairs enable partitioning of the stratigraphic column into layers for use in the decompaction process. Lithologic interpretations based on well log interpretations and core samples allow generalization of lithologic properties within each layer. Porosity is calculated from sonic log results. Corrected bore hole temperatures, vitrinite reflectance measurements, and drill stem test pressure measurements serve as constraint for the temperature, organic maturity, and pore pressure models. Chapter 4 summarizes the results of the modelling.

CHAPTER 4 MODEL RESULTS

4.1 Introduction

This chapter presents model results obtained using the data of Chapter 3. Because the modelling process is interactive, meaning that parameters can be changed easily to test various hypotheses, the results of the models are also interpretations. This chapter outlines the results of the preferred models and explains the assumptions and reasoning that led to them. Chapter 5 discusses these results in greater detail and proposes alternatives to the models discussed in this chapter.

4.2 Burial History

Burial history plots resemble the subsidence histories generated by various rift models (McKenzie 1978; Beaumont et al. 1982; Keen and Beaumont 1990), however burial histories cannot be interpreted as subsidence histories because of the effects of variable sedimentation rates. For example, the mid-Cretaceous, between 115-95 Ma, is a time of slow burial (Fig 4.1). The calculated burial history is unable to discern whether this is the result of low subsidence rate or low sediment input. This study does not attempt to separate the effects of subsidence rate and sediment input; it only considers compaction effects on the sediments.

Figure 4.1 presents the results of the decompaction procedure described in Section 2.1.2 as a graph of burial history through time. Each line on the graph represents the burial depth of the bottom of a unit through time. For example, the lowermost line corresponds with the bottom of unit 25; the one above is the Egret Member.

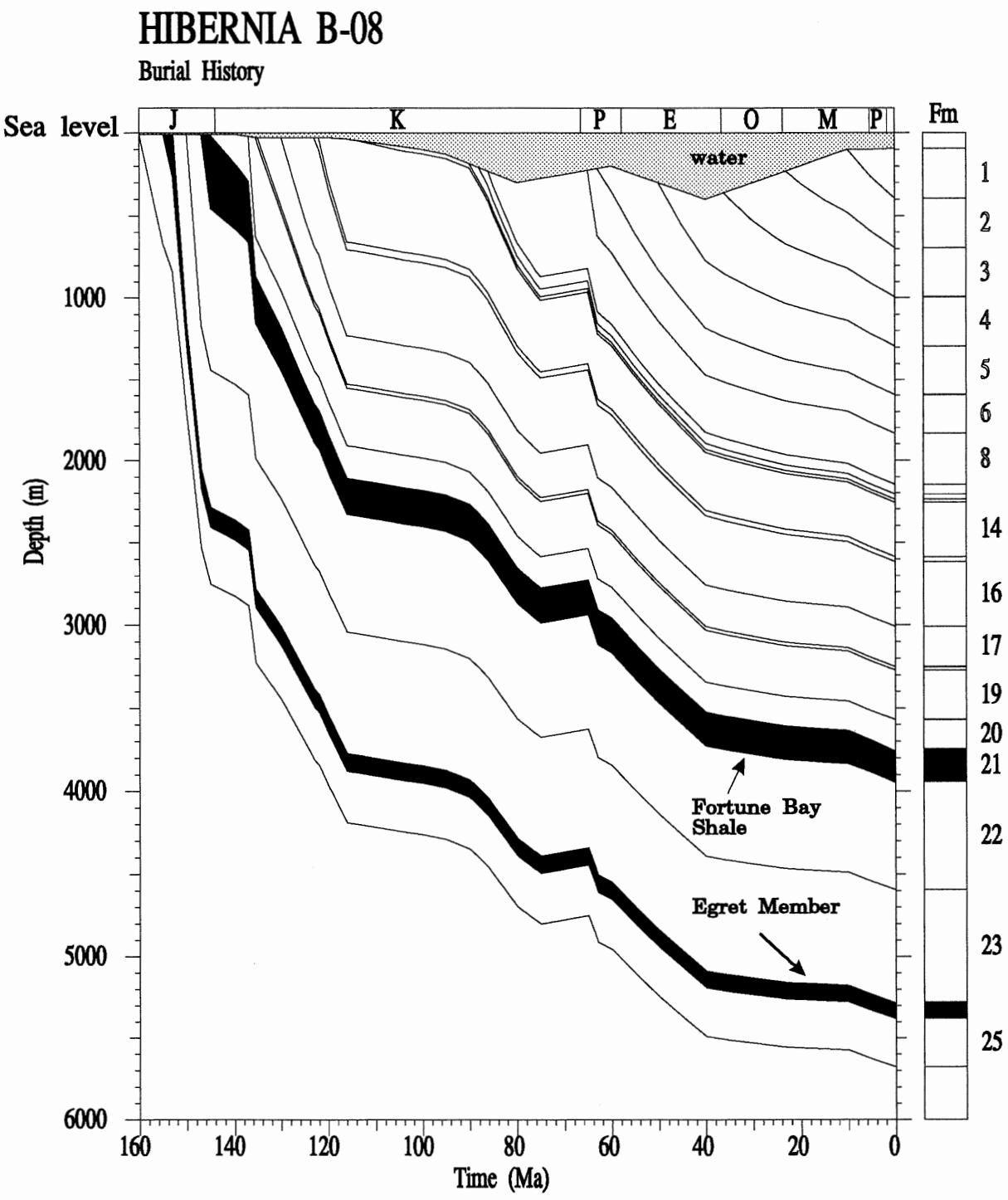

Figure 4.1 Burial history curve for preferred model (for model parameters see Appendix B). Each line represents the change in depth of a stratigraphic unit through time. The Egret Member is the source rock for hydrocarbons found in the Hibernia field, and the Fortune Bay Shale is the capping unit for the overpressures (see text).

Sedimentation rates are generated by dividing the decompacted thickness of the unit by the duration of deposition within it. Sharp peaks in sedimentation rate may be artifacts of irregular distribution of paleontological data in the well. Periods of apparent constant deposition may represent sharp pulses and lapses in sedimentation averaged out over the time interval considered. Therefore, small-scale details in the sedimentation rate curve may indicate real changes, but the actual values for the intervals should be considered approximations.

The general pattern in Figure 4.1 is one of rapid initial burial in the Late Jurassic (from 160 Ma to 120 Ma) followed by slower rates through the Cretaceous and Cenozoic. Periods of steep increases in sedimentation rate punctuate this trend at about 155, 136, and 64 Ma (Fig. 4.2). Rapid subsidence, enabling greater sediment accumulations, or increased sediment input into a steadily subsiding basin may cause these increases.

Limited knowledge of the biostratigraphy is of particular importance in the Cenozoic section of the Hibernia field. Little paleontologic data above 1500 m limits the resolution of sedimentation rates in this interval.

4.3 Temperature and Hydrocarbon Kinetics

Calculating results from the thermal model described in Section 2.1.3 requires selecting a heat flow value for Equation 2.3. Laboratory measurements constrain thermal conductivity values (Table 3.3), enabling calculation of thermal gradient. The quality of fit between measured and predicted temperature and vitrinite reflectance determines the preferred heat flow value.

The VITRIMAT technique applies constants to describe reactions within the source rock (Burnham and Sweeney 1989). Each set of constants determines the results of the reaction rate

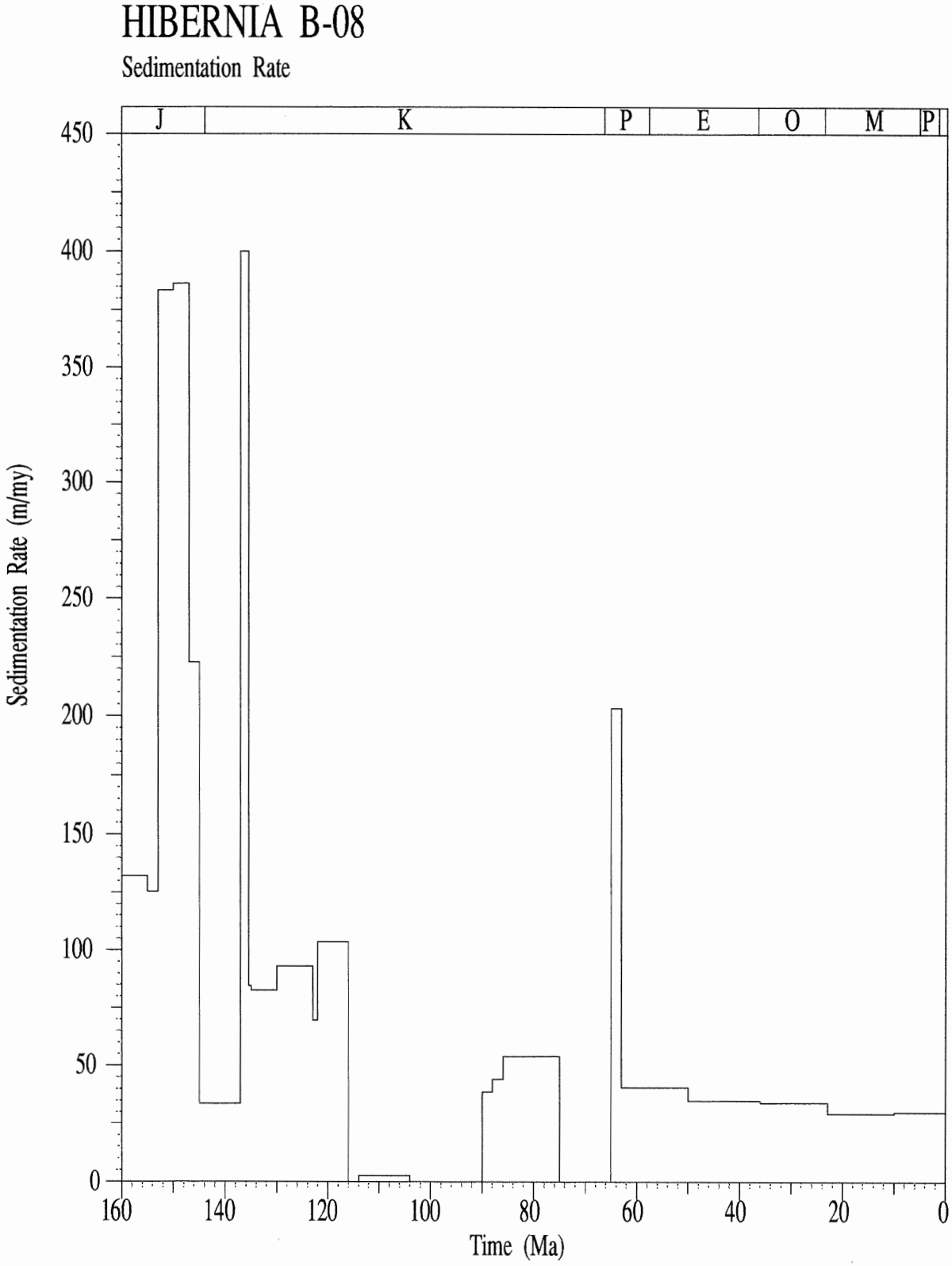

Figure 4.2 Sedimentation rate through time for Hibernia B-08.

equation (Eqn. 2.13). Thermal conductivity and heat flow values determine the temperature within the unit. Integrated with the reaction rate equation in VITRIMAT, these determine the degree of organic maturation (Sweeney and Burnham 1987).

Figure 4.3 shows the results of temperature and vitrinite reflectance predictions compared with measured temperatures and vitrinite reflectances, for a constant heat flow value of 35 mW/m^2. Model predictions do not use the observed BHT's and vitrinite reflectance measurements in the computation; the observed values are only plotted for comparison.

The heat flow selected for the model need not be constant. Many rift models predict a heat flow pulse at, or shortly after, the time of rifting; however, the magnitude of the pulse decays rapidly (Keen and Beaumont 1990). Recent modelling of crustal stretching on the Grand Banks shows that minor thinning occurred in the Jeanne d'Arc basin, and that only a small thermal pulse would result (Keen et al. 1987). The thermal pulse associated with the opening of the Atlantic later in the Jurassic would probably have had little effect on the Jeanne d'Arc basin, because the basin is located off of the axis of the main rift (Keen et al. 1987). Also, because initial rifting of the Jeanne d'Arc basin in the Late Triassic preceded deposition of the sediments drilled at Hibernia B-08 by approximately 60 Ma, the thermal pulse should have dissipated enough that a constant heat flow is probable over the last 160 Ma (Williamson in press).

The heat flow used in Figure 4.3 is the preferred choice for this data set. Even so, it underestimates the thermal gradient below about 2500m. Higher heat flow estimates better reproduce deeper temperatures, but overestimate shallower values and overestimate organic maturity. This problem is discussed more completely in Appendix A.

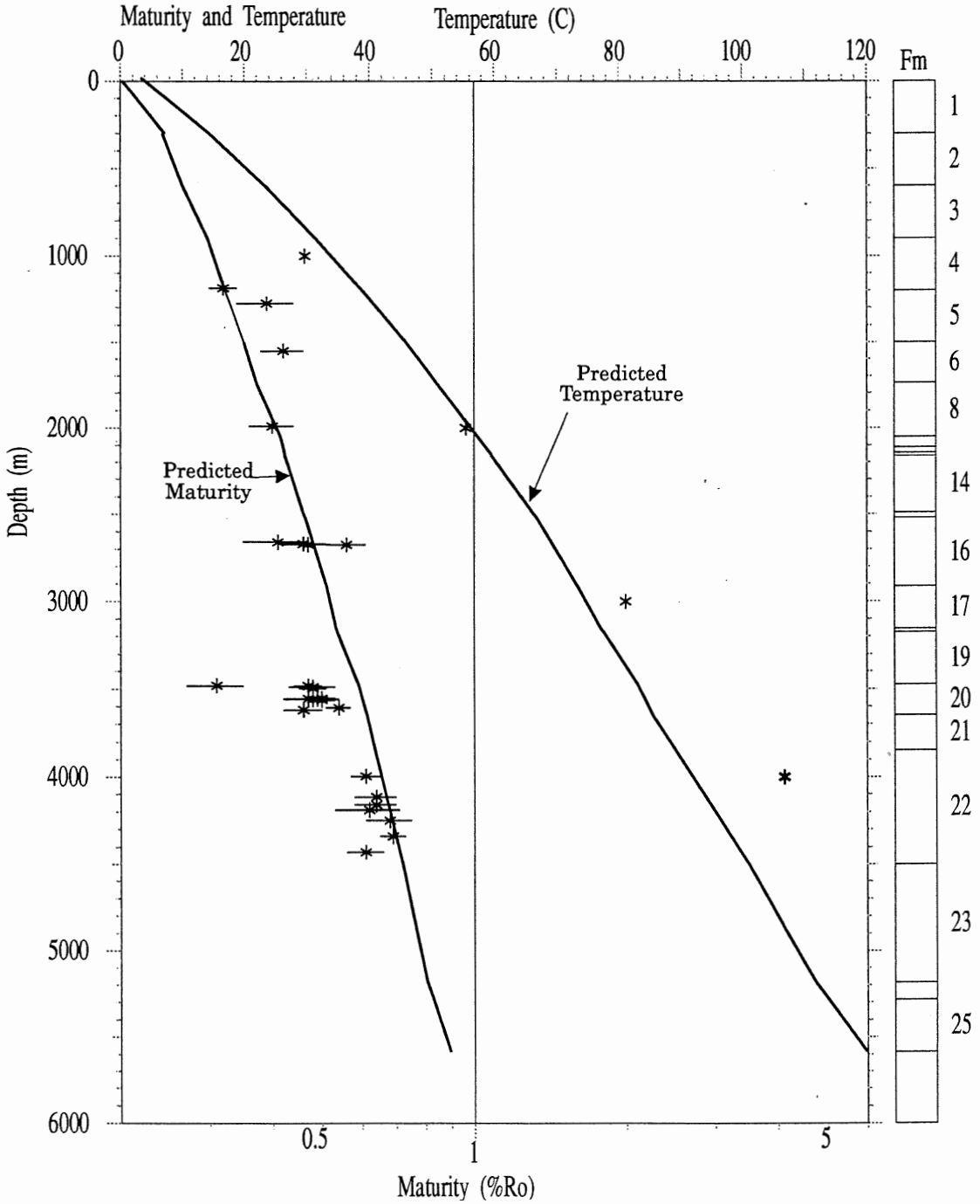

Figure 4.3 The results of temperature and vitrinite reflectance predictions compared with measured temperatures and vitrinite reflectances, for a constant heat flow of 35 mW/m^2. Stars are corrected BHT's and stars with line are measurements of vitrinite reflectance, with associated error bar. This model uses Set 1 thermal conductivity (Correia et al. 1989) values and a heat flow of 35 mW/m^2. The measurements are not used in the modelling; they are plotted to test the fit of the heat flow.

Figure 4.4 shows the maturation of the Egret Member through time. The plot is a compilation of maturity predictions for each decompaction interval. Rapid early subsidence in the first 20 my after deposition caused rapid maturation of the source rocks. After approximately 115 Ma, the unit gradually increases in maturation to the present. The horizontal line at $\%R_o = 0.70$ represents the onset of major oil generation which occurs at 70 Ma.

4.4 Pore Pressure

Figure 4.5 shows modelled and measured pore pressures. Pore pressure measurements show overpressuring at 3600 m depth. The modelled pressure underestimates the amount of excess pressure measured. This may imply that other factors not taken into account in the pressure model, such as hydrocarbon generation, or shale dewatering, have affected pressure development in the area. This possibility is discussed in greater detail in Chapter 5.

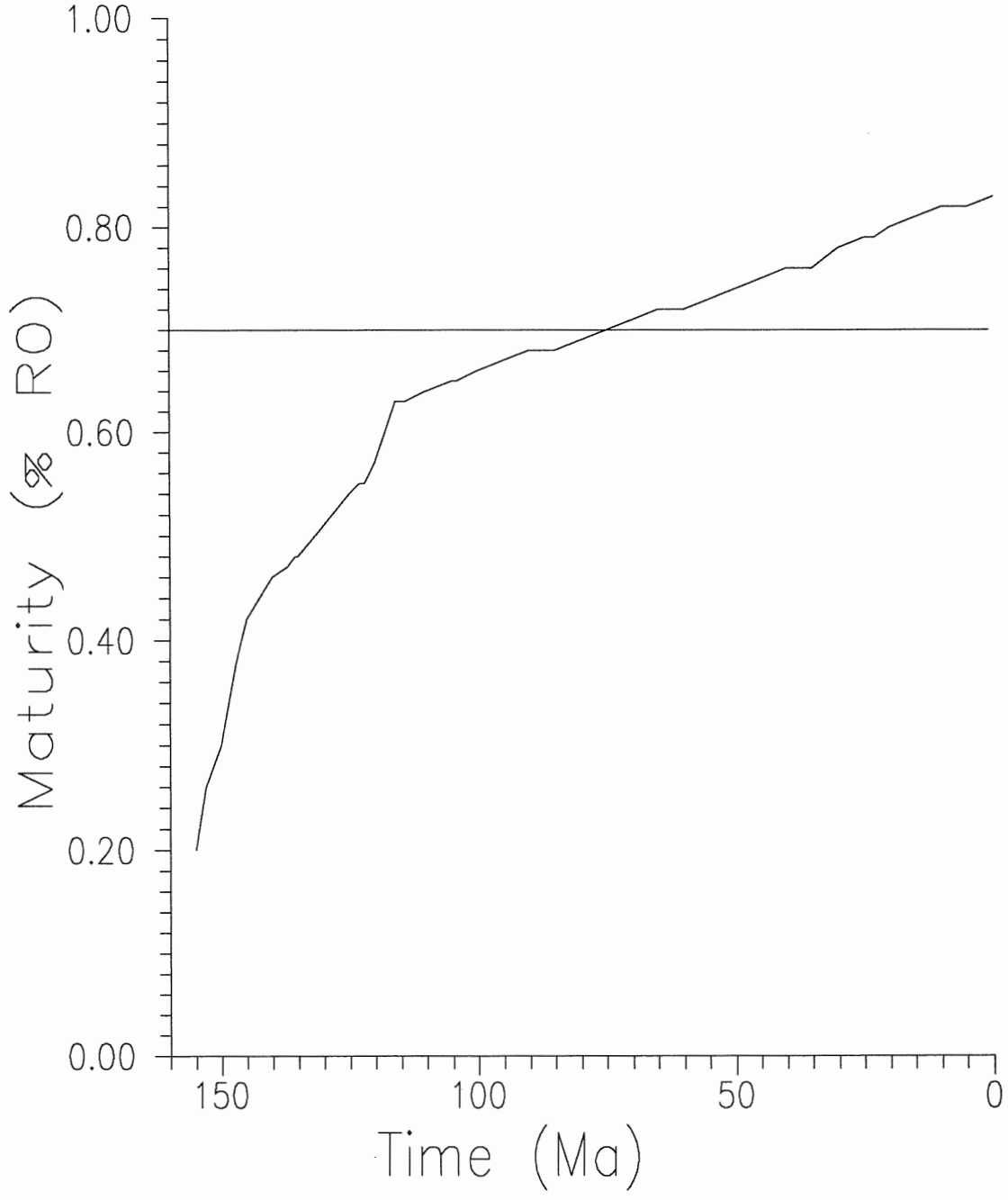

Figure 4.4 Plot of maturity development through time for the Egret Member. The horizontal line at $\%R_o$= 0.70 represents the onset of major oil generation.

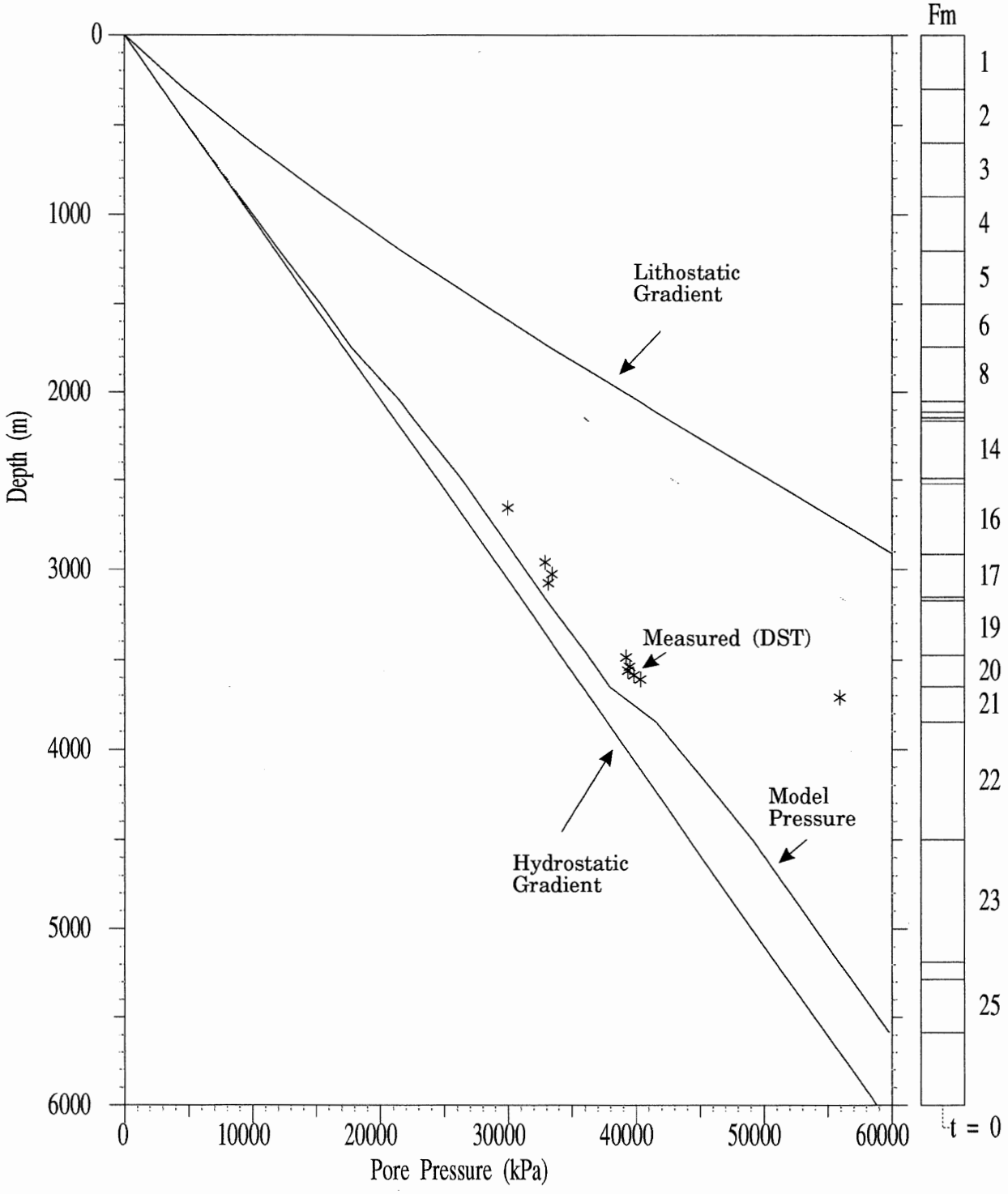

Figure 4.5 Plot of modelled and measured pore pressure. See Section 1.4 for description of terminology.

4.5 Summary

Burial history plots show rapid burial in the Late Jurassic and Early Cretaceous, decaying rapidly to lower levels. Slow burial rates continue throughout much of the Cenozoic. Results of thermal modelling show that a constant heat flow of 35 mW/m^2 adequately reproduces measured temperature and organic maturity. Pore pressure models do not predict the extensive overpressures found beneath the Fortune Bay Shale. Chapter 5 discusses these results with respect to organic maturity timing and pore pressure generation mechanisms.

CHAPTER 5 DISCUSSION

5.1 General

As discussed in Chapter 2, interpretations based on the techniques used in this study rely on the quality of the assumptions made in the model. This chapter is a discussion of the results of the models presented in Chapter 4.

5.2 Causes of Overpressures

5.2.1 General

Overpressures are common in many hydrocarbon-producing basins (Fertl 1976). The cause of overpressuring has been attributed to various mechanisms, including rapid sedimentation, thermal expansion of water, hydrocarbon generation, shale mineral transformations, and osmotic flow (Bradley 1975; Fertl 1976; Chapman 1980; Shi and Wang 1986; Demin 1988). The following sections briefly outline the characteristics of these mechanisms; a discussion of their significance to pressure development in the area of Hibernia B-08 follows.

5.2.1 Rapid sediment loading

Burial compaction results in porosity loss and pore fluid expulsion. Periods of rapid sedimentation cause rapid subsidence and compaction. During periods of fast deposition, compaction and fluid expulsion occur more quickly. Overpressures develop under these conditions when a restriction inhibits fluid expulsion (Fertl 1976). Shales commonly provide this low permeability cap.

5.2.2 Thermal overpressures

Because the thermal expansion of water is greater than that of sediments, pore fluid volume will increase more rapidly than grain volume with burial (Bradley 1975). During burial, as a unit is exposed to higher temperatures, excess pressure will result. To generate overpressures effectively, the cap rock must be impermeable enough to resist fluid volume increases of 0.5%, or less (Chapman 1980) and the porosity must remain constant during burial. The model is that of a rigid framework of grains that resists the thermal expansion of water and results in overpressure development.

Several authors argue that these are not geologically reasonable considerations, that even the most impermeable shales allow some flow (Chapman 1980; Shi and Wang 1986), and that rock porosity varies with effective stress (Shi and Wang 1986). Also, under geologically reasonable subsidence rates and permeabilities, the rate of thermal expansion is slow enough that most of the pressure will seep off as it develops (Chapman 1980). For these reasons, the models presented here do not consider the thermal expansion of pore fluids as a means of generating overpressures.

5.2.3 Shale mineral transformations

Shale mineral transformations, most commonly the conversion of smectite to illite, result in the expulsion of up to 20% of the shale volume as water (Bruce 1984). The temperature range over which smectite-illite transformations occur varies from 70-165 °C, depending on exact mineralogy (Bruce 1984). Typically, the depth interval over which this transformation takes place varies from 2000-3500 m (Bruce 1984). Shale transformations play an important role in the

important role in the migration of hydrocarbons, and are important producers of overpressures (Bruce 1984).

5.2.4 Hydrocarbon generation

The conversion of kerogen to liquid hydrocarbons adds considerable quantities of water, hydrocarbons, and volatile gases such as carbon dioxide to pore fluids. These fluids can generate overpressures in low permeability reservoirs if gas generation exceeds the rate at which fluids are expelled from the reservoir (Law and Dickinson 1985).

5.2.5 Osmotic pressure

Osmotic flow can occur where a semi-permeable membrane separates two solutions of different concentrations. In geological environments, low permeability shales provide the membrane, and pore water of varying salinity, the solutions (Fertl 1976). Most workers consider osmotic pressure to be a possible secondary source for overpressuring, but not generally important as a primary pressure mechanism (Shi and Wang 1986; Mudford 1988). At present it is not possible to model osmotic pressure generation because osmotic pressures in geologic settings are poorly understood (Ungerer et al. 1990). Therefore, this study does not consider osmotic pressure as a contributor to pore pressure development.

5.3 Hydrocarbon Generation

Figures 4.3 and 4.4 present the results of organic maturation models using Set 1 thermal conductivity values (Correia et al. 1989) (Table 3.3) with a constant heat flow of 35 mW/m^2. This set of parameters predicts the organic maturity of the Egret Member to have reached $\%R_o$= 0.70 at about 70 Ma, similar to predictions made by Williamson (in press). Geologically reasonable changes to compaction factor and surface porosity values have no appreciable affect on this result (Appendix A). The maturation timing is, however, sensitive to variability in thermal conductivity (Appendix A).

5.4 Pressure Discussion

As discussed in Section 2.1.4, the modelling techniques used in this study allow overpressure generation by compaction effects, but neglect others, including hydrocarbon generation and shale mineral transformations. Measured pore pressures indicate that overpressuring occurs at a depth of 3600 m (Fig. 4.5), in the Fortune Bay Shale (Unit 21) (Fig. 1.2). The model presented in Figure 4.5 produces a small pressure increase at this level, indicating the Fortune Bay Shale is a seal for modelled overpressures, but the units beneath do not generate enough pressure to fully overpressure the unit.

This underestimation suggests that, while compaction may contribute to overpressuring, it is not responsible for all of the measured pressure of the well. The consistently low sedimentation rates determined for the last 60 Ma also suggests that rapid sedimentation is not the main overpressuring mechanism (Fig. 4.2). Higher recent sedimentation rates might be expected to generate greater pressure in the model. More detailed study of the biostratigraphy of the Cenozoic

strata in the Hibernia field may lead to a better understanding of the sedimentation patterns and rates. This, in turn, may change the pore pressure model proposed here.

Although the modelling technique adopted in this study cannot quantitatively estimate the effects of other overpressuring mechanisms, some general observations do apply to the nature of overpressures in the area. Integrating results from the maturity development model (Fig. 4.4) and burial history curve (Fig. 4.1) allows discussion about the relative importance of smectite-illite transformation and hydrocarbon generation as pressure generating mechanisms.

Smectite to illite transformation takes place over depths ranging from 2000-3500 m (Bruce 1984). Burial of the stratigraphic units beneath the Fortune Bay Shale was rapid enough in the Late Jurassic and Early Cretaceous that all units were buried below 2000 m before 120 Ma, and below 3500 m before 40 Ma, indicating that if shale mineral transformations are the major source of overpressure, the fluid regime had to be maintained for 40 to 120 Ma.

Figure 5.1 is a plot of porosity and permeability development through time in the Fortune Bay Shale. At 60 Ma, the porosity of the unit is over 10% and its permeability is 10^{-2} md. Permeability in shale varies from 10^{-1} md (Brace 1980) to 10^{-18} md (Katsube et al 1991). Therefore, these values are near the upper limit for shales. By the present day, however, the porosity has decreased to 5% and the permeability has decreased to 0.002 md, low enough to begin forming an effective trap (Mudford and Best 1989). It is likely, therefore, that the Fortune Bay Shale only became an important pressure cap in the last 60 Ma. That the Fortune Bay Shale only becomes an effective trap after the bulk of the shales beneath it have undergone smectite-illite transformation argues against such transformations being the major pressuring mechanism.

Figure 4.4 shows that at approximately 60 Ma the Egret Member began generating large

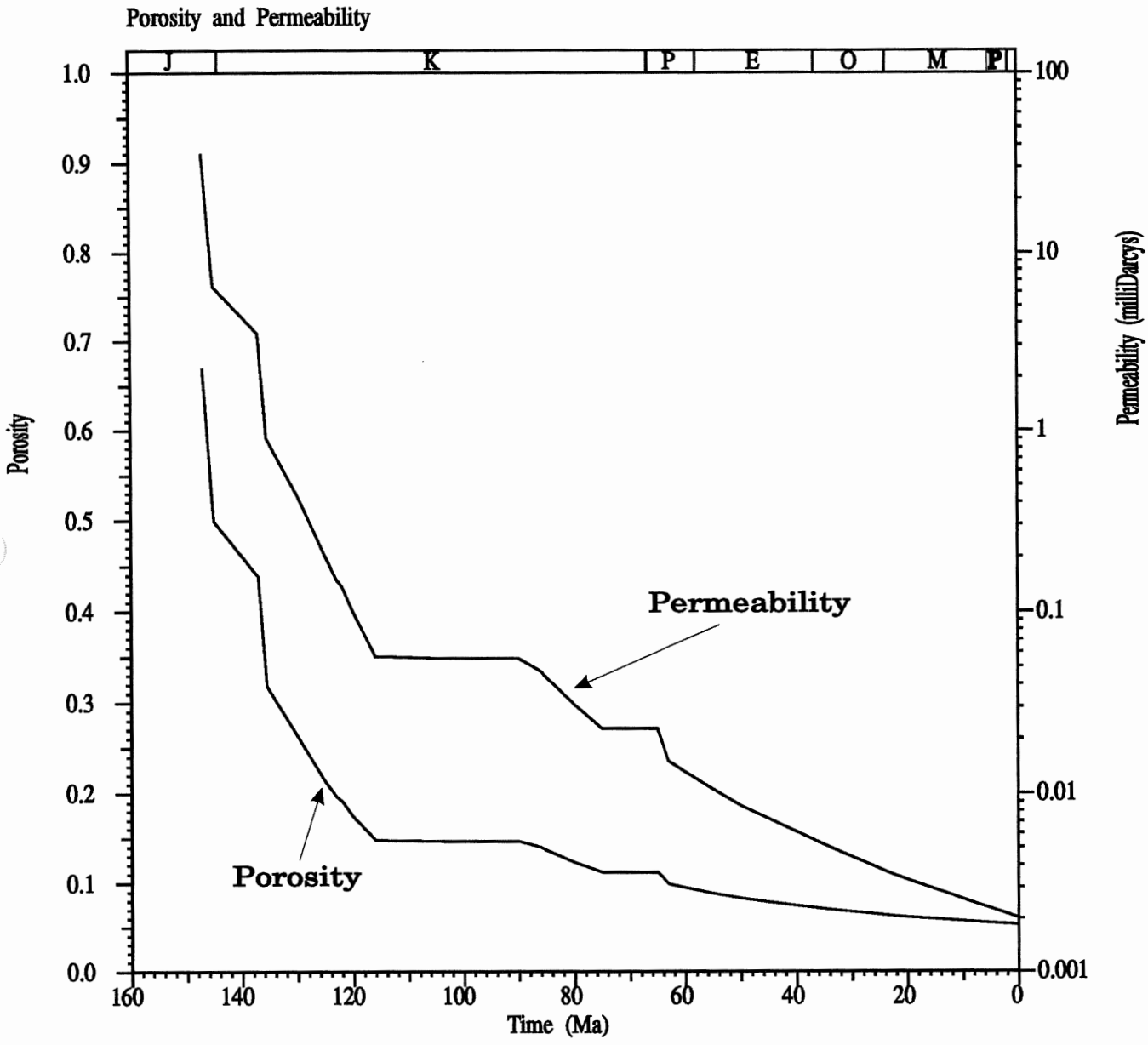

Figure 5.1 Plot of the development of porosity and permeability through time for the Fortune Bay Shale. Note the steady decrease in permeability in the last 60 Ma. See discussion in text.

quantities of hydrocarbons. The figure also shows that the unit is still within the oil window and is, therefore, still generating hydrocarbons. Qualitatively, it is possible to say that hydrocarbon generation is a potential mechanism by which the overpressures in the well have developed. Models exist to test this hypothesis (Mudford and Best 1989), but such calculations are beyond the scope of the present study.

CHAPTER 6 CONCLUSIONS

6.1 Summary

Through the integration of a broad range of physical, chemical, and geological data, this study has derived an understanding of the compaction, subsidence, thermal, organic maturity, and pressure history of the Hibernia B-08 well. Given the assumptions made to derive the models (see text for discussion), the results of the modelling show:

1 An initial very rapid sedimentation and compaction rate from 160 Ma to 120 Ma.

2 Present-day heat flow in the Hibernia B-08 well is 35 mW/m^2, and may have been approximately constant as a result of its off-rift location. Any thermal pulse associated with the original rift in the Triassic would have dissipated before deposition of any units in this section.

3 Oil generation in the Egret Member began at 75 Ma and continues to the present day.

4 Abnormal pore pressures began to accumulate during the last 60 Ma, because prior to this time the capping Fortune Bay Shale was too permeable and not an effective seal.,

5 Consistent, low deposition rates in the last 60 Ma result in minor development of compaction-driven overpressure.

6 Smectite-illite transformation as a mechanism for generating overpressure is unlikely because of rapid burial in the Late Jurassic and Early Cretaceous. This early rapid burial resulted in rapid compaction to beneath the bottom of the shale mineral transformation depth. The most likely mechanism for overpressuring, therefore, is hydrocarbon generation

from the Egret Member.

7 Sensitivity analysis of some of the assumptions show that the timing of hydrocarbon generation may vary by 40 Ma (from 70 to 110 Ma), depending on the thermal conductivity values used.

6.2 Recommendations for Further Study

Further studies of this nature in the Jeanne d'Arc basin should focus on the volumetric output of the hydrocarbon sources. The scientific benefits would be twofold. First, this would enable more accurate prediction of hydrocarbon reserves in the Hibernia field. Second, an understanding of the hydrocarbon output would allow more accurate modelling of the overpressures using the methods of Mudford and Best (1989). Also, sensitivity studies that enable further constraint of petrophysical parameters such as grain size, permeability, and thermal conductivity would improve the accuracy of the models presented here. Such studies might include the use of techniques to interpret petrophysical parameters from well logs, for example the technique of Brigaud et al. (1990) that determines thermal conductivity from well log information (Huang and Williamson, in preparation).

APPENDIX A SENSITIVITY ANALYSIS OF MODEL ASSUMPTIONS

A.1 Introduction

The purpose of a sensitivity analysis is to study the role of assumption on the models (see text for discussion). The purpose of this section is to present a few figures showing the effects of uncertainty in some assumptions on the output of the model. Because of their importance, the parameters tested are the thermal conductivity, compaction factor, and grain size.

A.2 Thermal Conductivity

The thermal and hydrocarbon kinetic models presented above use Set 1 thermal conductivity values. Because the Set 2 thermal conductivity values are from a different area (Scotian Shelf), they are only considered for comparison purposes. For convenience, Model 1 will refer to the thermal model using the first thermal conductivity set, and Model 2, the second.

In Model 1 the heat flow needed to match the thermal and vitrinite reflectance profiles is 35 mW/m^2. A heat flow of 28 mW/m^2 generates a similarly good fit to the data when in Model 2 (Fig. A-1). This is the result of higher average thermal conductivity values at depth in Model 1. Higher thermal conductivities allow more heat to escape, therefore a higher heat flow is necessary to maintain the same temperature gradient .

The hydrocarbon kinetic model was used in Chapter 5 to predict the onset of oil generation. Figure A-2 compares the timing of oil generation using the two conductivity sets. Model 1 reaches $\%R_o$ = 0.70 at 75 Ma and 0.80 at 20 Ma. Model 2 reaches $\%R_o$ = 0.70 at 105 Ma and $\%R_o$ = 0.80 at 35 Ma. Without control on the thermal conductivity values, predictions of the onset of oil generation could vary by as much as 30 Ma.

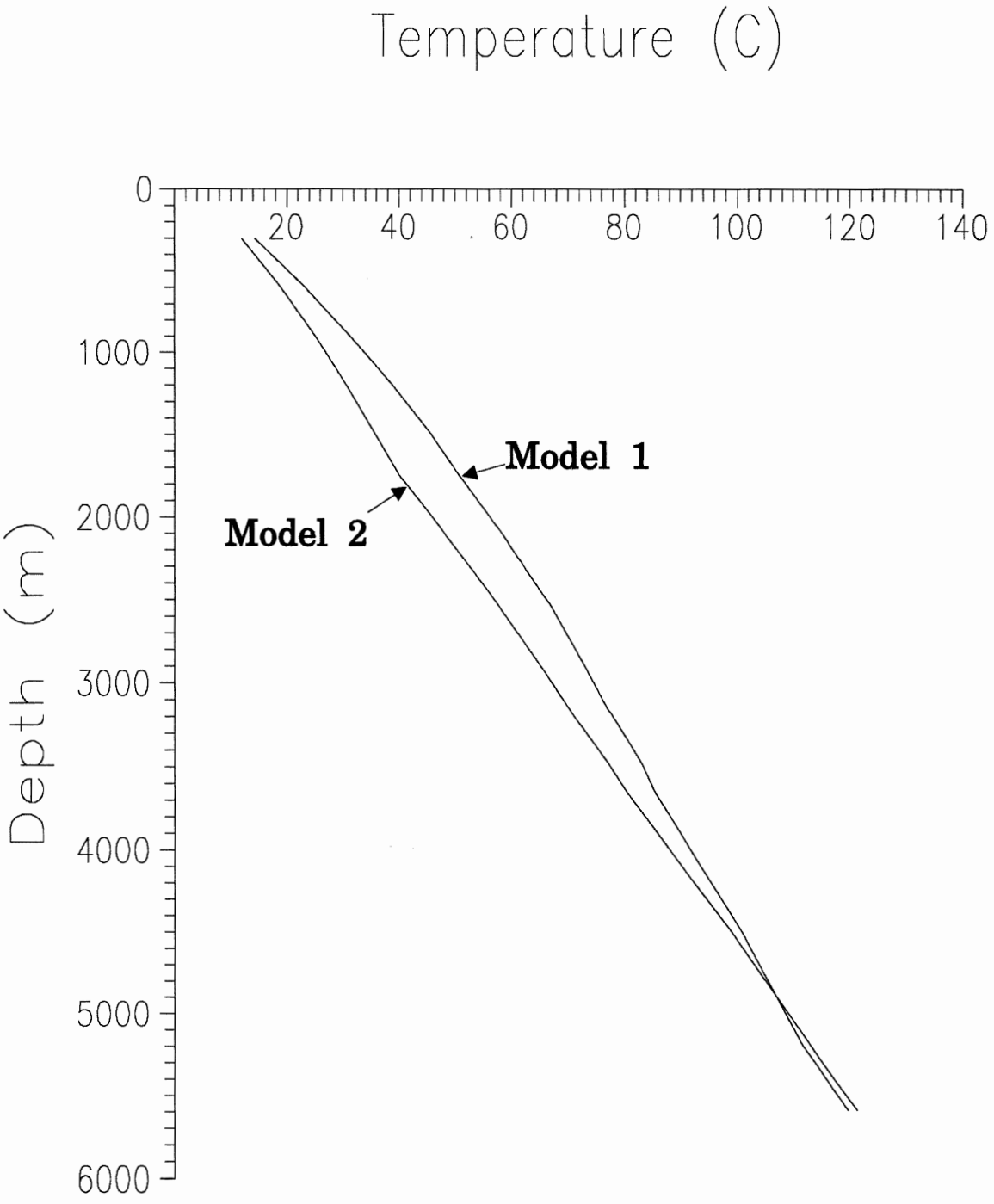

Figure A.1 A plot of temperature gradients for Model 1 and 2. Model 1 uses a heat flow of 35 mW/m^2 and model 2, 28 mW/m^2.

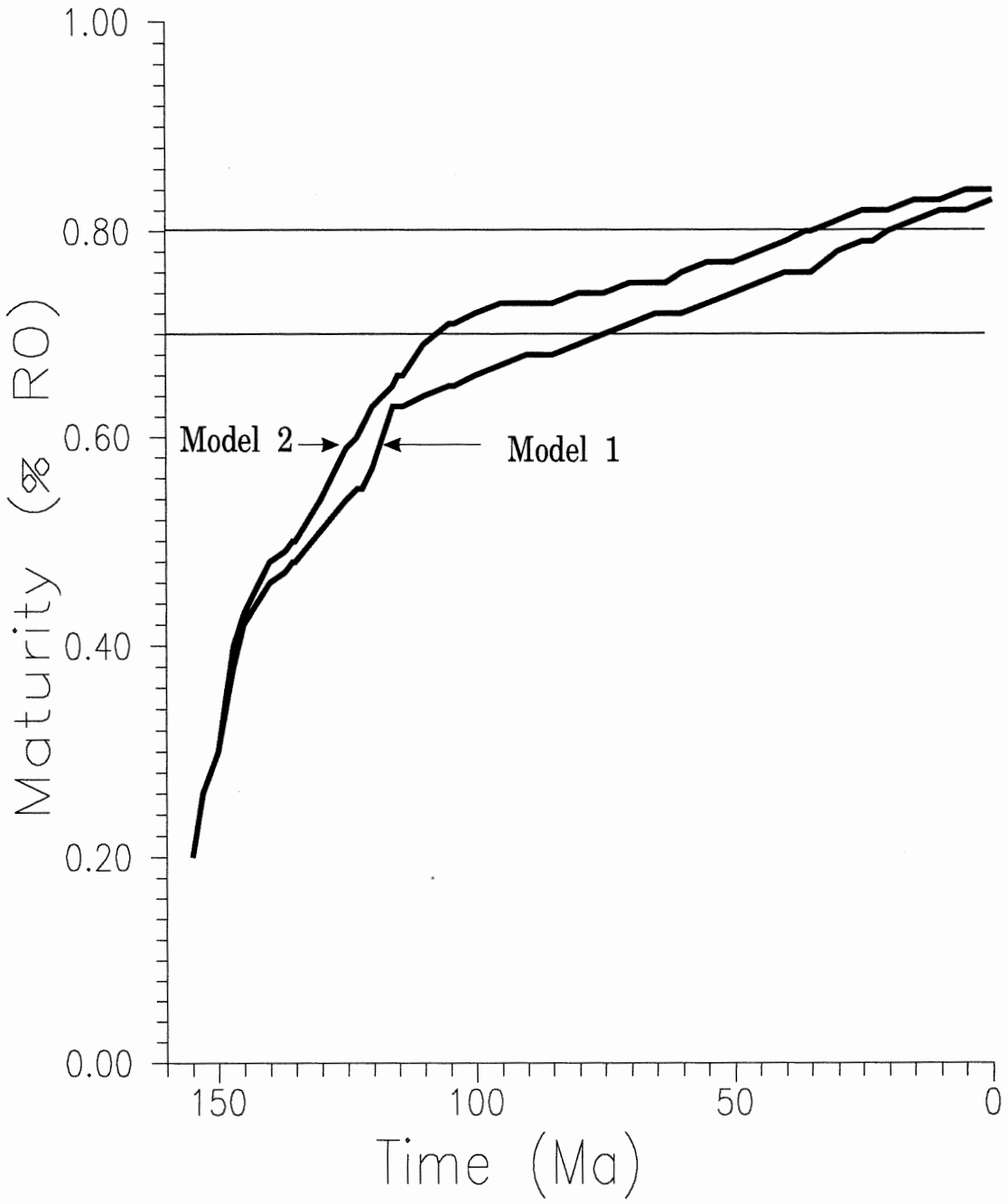

Figure A.2 A plot of maturity development through time for the Egret Member, using both models. See text for discussion.

A.3 Compaction Factor

The porosity-depth curve controls many of the models generated above. Figures A.3 and A.4 demonstrate the effects of compaction factor on pressure and permeability. Lower compaction factors generate higher permeabilities (Fig. A.3), and lower pressures (Fig A.4). In the present study, a variation of 10% in compaction factor results in a doubling in the permeabilities (Fig. A.3), but only moderate changes in pore pressure (Fig A.4). If compaction effects were the main mechanism for overpressuring, porosity variation should have a much more profound effect on the pressure model.

A.4 Grain Size

Figures A.5 and A.6 show that as grain size decreases, pressure increases. This is the result of the derivation of the Kozeny-Carmen equation (Eqn. 2.6) with respect to mean grain diameter (Eqn. 2.8). the effects are greater for shales than for sandstones because shales are more likely to have low enough permeability to enable pressure development.

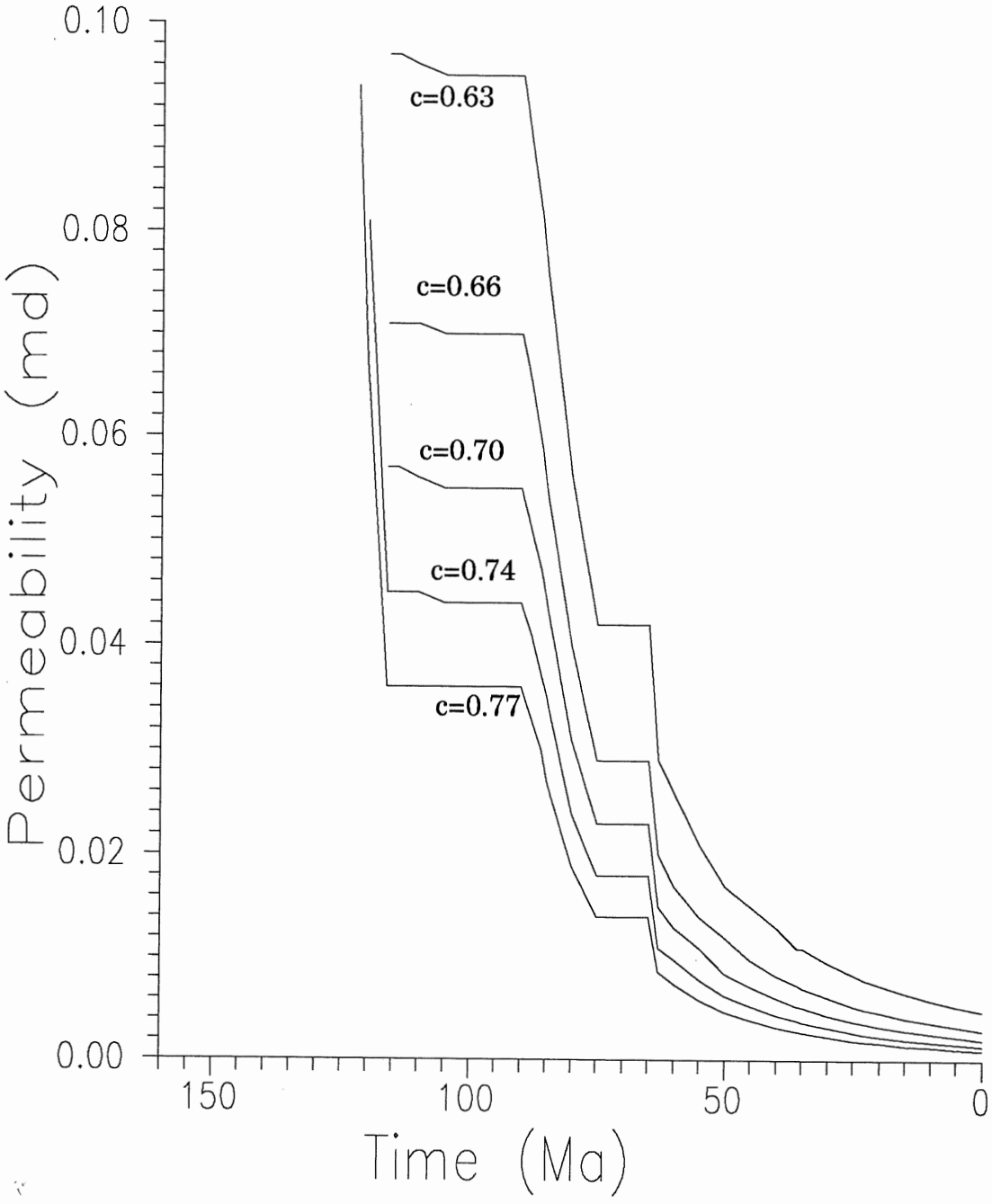

Figure A-3 Permeability development through time for various compaction factors (c). Higher factors correspond to faster porosity and permeability loss with depth. Compare with figure A-4.

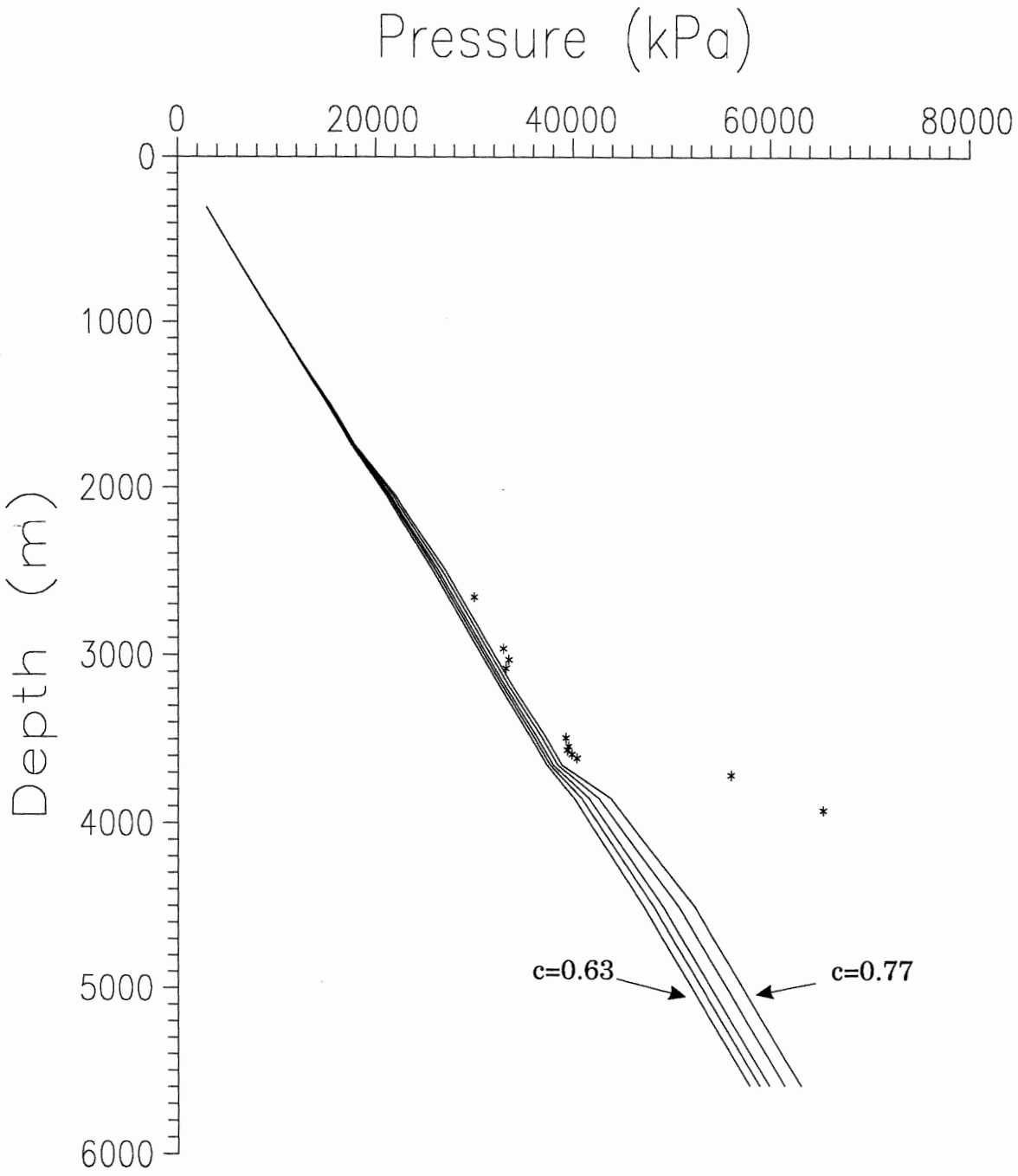

Figure A-4 Pressure versus depth showing the correlation between high compaction factor (c) and high pressure predictions.

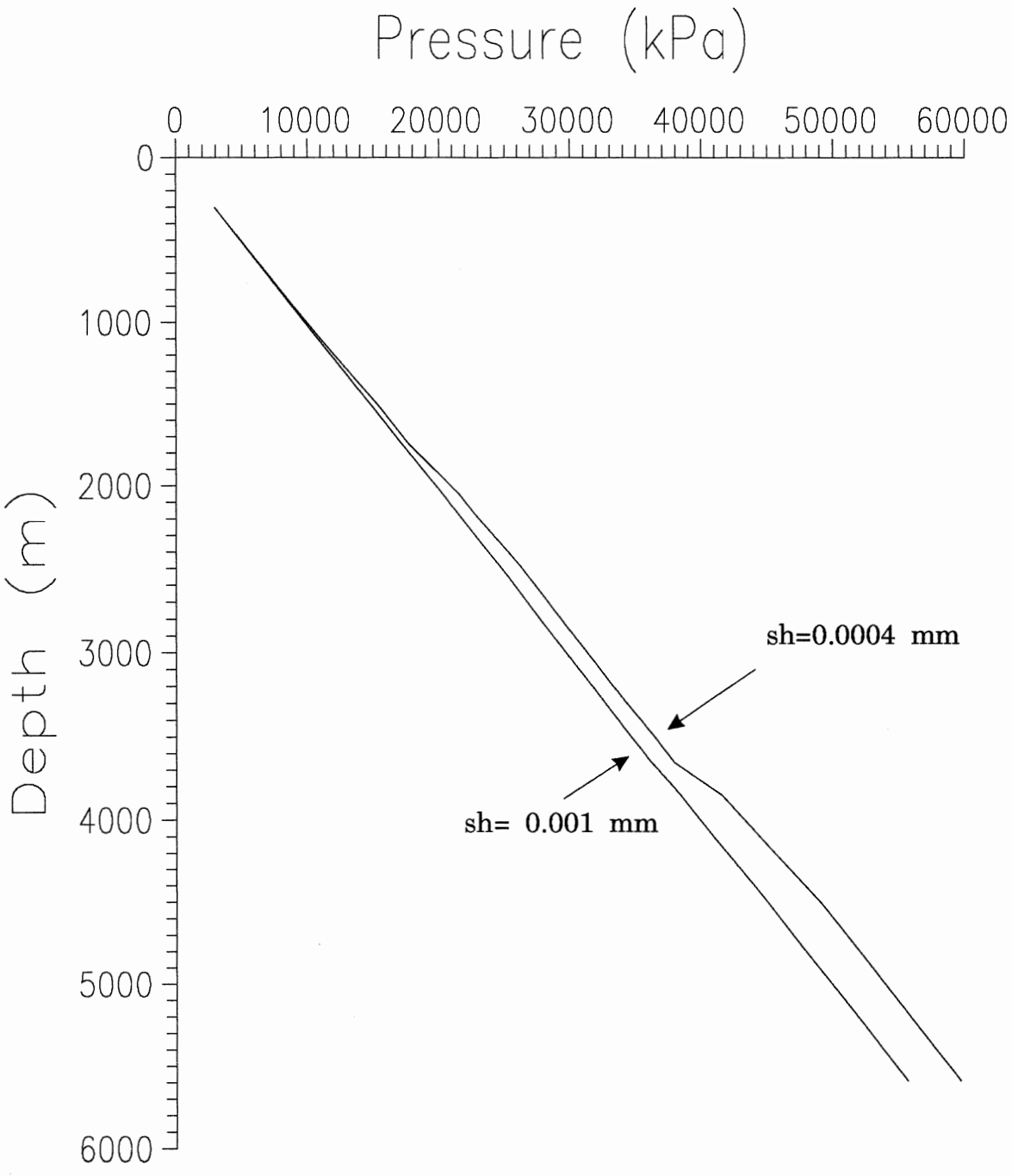

Figure A-5 Pressure predictions using different shale grain sizes (sh). As expected, lower grain sizes result in higher pressure predictions. Compare with figure A-6.

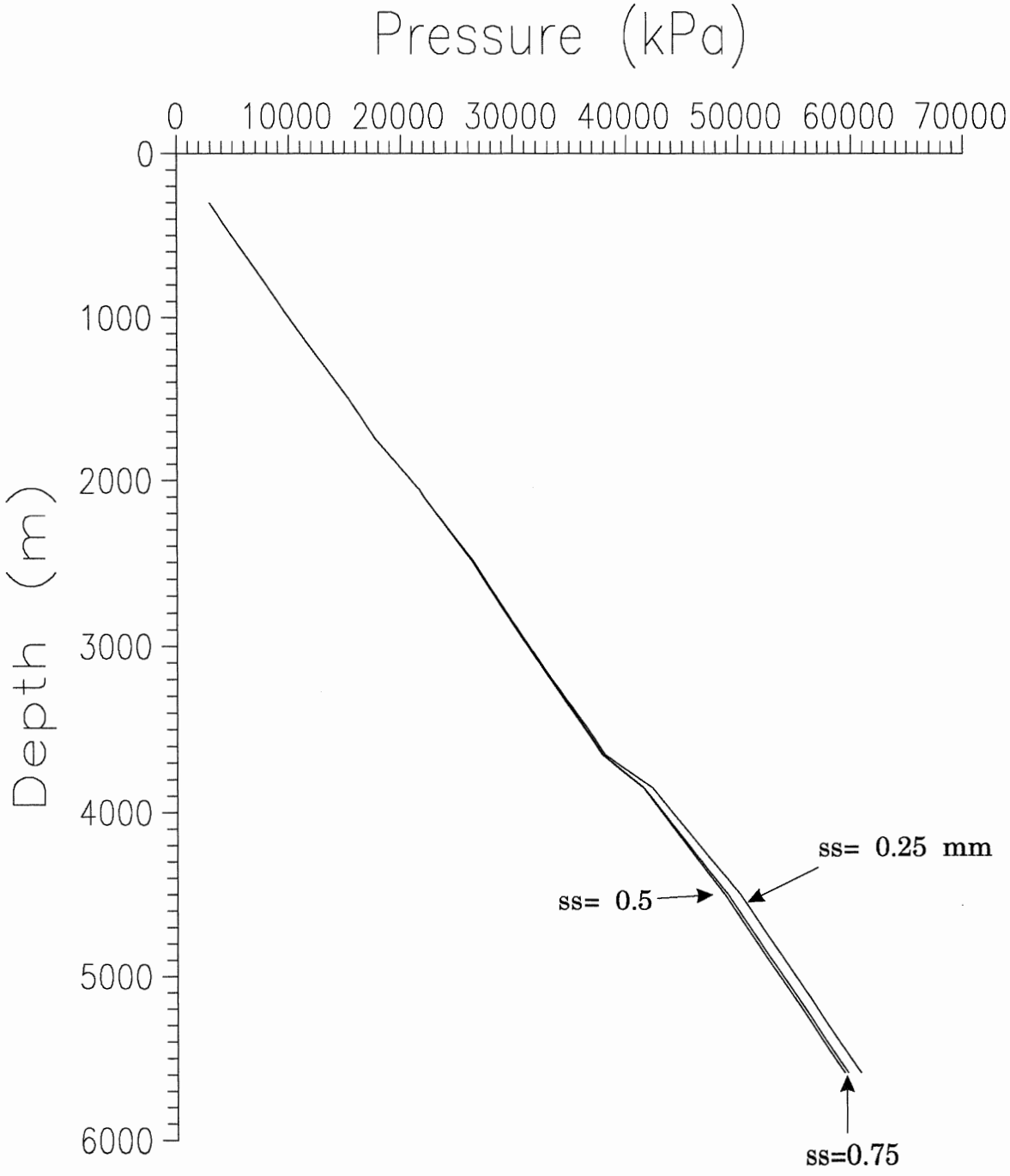

Figure A.6 Pressure models showing the effect of varying the sandstone grain size parameter (ss). note the small variation compared to figure A.5.

References

Ascoli P (1983) Report on the ostracod biostratigraphy and depositional environments of the Mobil et al. Hibernia B-08, East Newfoundland Basin, from the top of the Cretaceous (1775 m) to 4165 m (TD 4435 m). Eastern Petroleum Geology Report, EPGS-PAL.23-82PA

Ascoli P (1988) Mesozoic-Cenozoic foraminiferal, ostracod, and calpionellid zonation of the North Atlantic margin of North America: Georges Bank-Scotian basins and northeast Grand Banks (Jeanne d'Arc, Carson, and Flemish Pass basins). Biostratigraphic correlation of 51 wells: Geol. Surv. Can. Open File Report 1791

Avery MP, Bell JS, McAlpine KD (1986) Vitrinite reflectance measurements and their implications for oil and gas exploration in the Jeanne d'Arc Basin, Grand Banks, eastern Canada. In: Current Res., Part A, Geol. Surv. Can., Paper 86-1A:489-498

Bear J (1972) Dynamics of Fluid Flow in Porous Media. American Elsevier, New York

Beaumont C, Keen CE, Boutilier R (1982) On the evolution of rifted continental margins: comparison of models and observations for the Nova Scotian margin. Geophys. J.R. astr. Soc. 70:667-715

Brace WF (1980) Permeability of crystalline and argillaceous rocks. Int. J. Rock Mech. Min. Sci. and Geomech. Abstr. 17:241-251

Bradley J (1975) Abnormal formation pressure. Am. Assoc. Petr. Geol. Bull. 59:957-973

Brigaud F, Chapman DS, Le Douaran S (1990) Estimating thermal conductivity in sedimentary basins using lithological data and geophysical well logs. Am. Assoc. Petr. Geol. Bull. 74:1459-1477

Bruce CH (1984) Smectite dehydration-Its relation to structural development and hydrocarbon accumulation in northern Gulf of Mexico Basin. Am. Assoc.Petr. Geol. Bull. 68:673-683

Burnham AK, Sweeney JJ (1989) A chemical kinetic model of vitrinite maturation and reflectance. Geochim et Cosmochim A. 53:2649-2657

Canadian Stratigraphic Services Ltd. (1982) Lithologic interpretations for well Mobil Hobernia B-08, Grand Banks of Newfoundland. Canadian Stratigraphic Services, Ltd.

Cathles LM, Smith AT (1983) Thermal constraints on the formation of Mississippi Valley-type lead-zinc deposits and their implication for episodic basin dewatering and deposit genesis.

Econ. Geol. 78:983-1002

Combarnous M, Bories S (1975) Hydrothermal convection in saturated porous media. Advances in Hydrosciences 10:231-307

Correia A, Jones FW (1991) The thermal regime in the Jeanne d'Arc basin, offshore eastern Canada. Tectonophys. 194:357-361

Correia A, Jones FW, Fricker A (1990) Terrestrial heat flow density estimates for the Jeanne d'Arc basin, offshore eastern Canada. Geophys. 55:1625-1633

Deming D, Chapman DS (1988) Inversion of bottom-hole temperature data: the Pineview field, Utah-Wyoming thrust belt. Geophys. 53:707-720

de Voogd B, Keen CE (1987) Lithoprobe east: results from reflection profiling of the continental margin: Grand Banks region. Geophys. J. R. astr. Soc. 89:195-200

Enechescu ME (1987) Tectonic and structural framework of the northeast Newfoundland continental margin. In: Basin Building Mechanisms. Can. Soc. Petr. Geol. Memoir 12:117-146

Falvey DA, Middleton MF (1981) Passive continental margins: evidence for a pre-breakup deep crustal metamorphic subsidence mechanism. In: Proceedings 26th International Geological Congress, Geology of the continental margins symposium, Paris, 7-17 July, 1980. Oceanol. Acta 4: 103-114

Fertl W (1976) Abnormal Formation Pressures. Elsevier, New York

Grant AC, McAlpine KD (1990) The continental margin around Newfoundland.In: Geology of the Continental Margin of Eastern Canada. Keen MJ, Williams GL (eds) Geol. Surv. Can., Geology of Canada no. 2 (also Geol. Soc. Am., The Geology of North America, v. 1-1) pp 239-292

Grant AC, McAlpine KD, Wade JA (1986) The continental margin of eastern Canada: geological framework and petroleum potential. In: Future Petroleum Provinces of the World. Halbouty MT (ed) Am. Assoc. Petr. Geol. Memoir 40: 177-205

Huang Z, Williamson MA (in preparation) The thermal structure of the Jeanne d'Arc basin.

Katsube TJ, Mudford BS, Best ME (1991) Petrophysical studies of shales from the Scotian Shelf. Geophys. 56:1681-1689

Keen CE, Beaumont C (1990) Geodynamics of rifted continental margins. In: Geology of the Continental Margin of Eastern Canada. Keen MJ, Williams GL (eds) Geol. Surv. Can.,

Geology of Canada no. 2 (also Geol. Soc. Am., The Geology of North America, v. 1-1) pp 391-472

Keen CE, Boutilier R, de Voogd B, Mudford BS, Enachescu ME (1987) Crustal geometry and models of the evolution of the rift basin on the Grand Banks of eastern Canada: constraints from deep seismic data. In: Sedimentary and Basin-Forming Mechanisms. Beaumont C, Tankard AJ (eds) Can. Soc. Petr. Geol., Memoir 12:101-115

Keen CE, Lewis T (1982) Measured radiogenic heat production in sediments from continental margin of eastern North America: implications for petroleum generation. Am. Assoc. Petr. Geol. Bull. 66:1402-1407

Magara K (1976) Thickness of removed sedimentary rocks, paleopore pressure, and paleotemperature,southwestern part of Western Canada Basin. Am. Assoc. Petr. Geol. Bull. 60:554-565

Law B, Dickinson W (1985) Conceptual model for origin of abnormally pressured gas accumulations in low-permeability reservoirs. Am. Assoc. Petr. Geol. Bull. 69:1295-1304

McAlpine KD (1990) Mesozoic stratigraphy, sedimentary evolution, and petroleum potential of the Jeanne d'Arc basin, Grand Banks of Newfoundland. Geol. Surv. Can. Paper 89-17: 50 pp

McKenzie D (1978) Some remarks on the development of sedimentary basins. Earth and plan. Sci. Letts. 40:25-32

Moir PN, Whidden JA (1989) The geothermal regime of the Grand Banks, offshore eastern Canada, from exploration well measurements. Geol. Surv. Can. Forum 1989, Oil and Gas Activities in Canada, Program with Abstracts:29

Mudford BS (1988) Modelling the occurence of overpressures on the Scotian Shelf, offshore eastern Canada. J. Geophys. Res. 93:7845-7855

Mudford BS, Best ME (1989) Venture gas field, offshore Nova Scotia: case study of overpressuring in region of low sedimentation rate. Am. Assoc. Petr. Geol. Bull. 73:1383-1396

Nakayama K, Van Siclen DC (1981) Simulation model for petroleum exploration. Am. Assoc. Petr. Geol. Bull. 65:1230-1255

Perrier R, Quiblier J (1974) Thickness changes in sedimentary layers during compaction history. Am. Assoc. Petr. Geol. Bull. 58: 507-520

Schlumberger (1979) Log interpretation charts: Schlumberger Ltd., New York

Sclater JG, Christie PAF (1981) Continental stretching: an explanation of the post-Mid-Cretaceous subsidence of the Central North Sea basin. J. Geophys. Res. 85:3711-3739

Shi Y, Wang Y (1986) Pore pressure generation in sedimentary basins: overloading versus aquathermal. J. Geoph. Res. 91:2153-2162

Smith JE (1971) The dynamics of shale compaction and evolution of pore-fluid pressures. Math. Geol. 3:239-263

Snowden LR, Fowler MG (1986) Rock-Eval/TOC data from seven wells located within the Jeanne d'Arc basin, offshore Newfoundland. Geol. Surv. Can. Open File Report 1382

Stecklar MS, Watts AB (1978) Subsidence of the Atlantic-type continental margin off New York. Earth Plan. Sci. Letts. 41:1-13

Sweeney JJ, Burnham AK, Braun RL (1987) A model of hydrocarbon generation from Type I kerogen: Application to Uinta basin, Utah. Am. Assoc. Petr. Geol. Bull. 71:967-985

Tankard AJ, Welsink HJ (1987) Extensional tectonics and stratigraphy of Hibernia oil field, Grand Banks, Newfoundland. Am. Assoc. Petr. Geol. Bull. 71:1210-1232

Tissot BP, Pelet R, Ungerer Ph (1987) Thermal history of sedimentary basins, maturation indices, and kinetics of oil and gas generation. Am. Assoc. Petr. Geol. Bull. 71:1445-1466

Ungerer P, Burrus J, Doligez B, Chenet PY, Bessis F (1990) Basin evaluation by integrated two-dimensional modelling of heat transfer, fluid flow, hydrocarbon generation, and migration. Am. Assoc. Petr. Geol. Bull. 74:309-335

van Hinte JE (1978) Geohistory analysis- application of micropaleontology in exploration geology. Am. Assoc. Petr. Geol. Bull. 62:291-322

Waples DW (1980) Time and temperature in petroleum formation: application of Lopatin's method to petroleum exploration. Am. Assoc. Petr. Geol. Bull. 64:916-926

Waples DW, Kamata H, Suizu M (1992) The art of maturity modelling. Part 1: finding a satisfactory geologic model. Am. Assoc. Petr. Geol. Bull. 76:31-46

Waples DW, Suizu M, Kamata H (1992) The art of maturity modelling. Part 2: alternative models and sensitivity analysis. Am. Assoc. Petr. Geol. Bull. 76:47-66

Williamson MA (in press) The subsidence, compaction, thermal, and maturation history of the Egret Member source rock, Jeanne d'Arc basin, offshore Newfoundland.